Fusion-Inducing Liposomes for Efficient Intracellular Delivery: Continuum Models and Experiments

Annalisa Quaini and Maxim Olshanskii

Department of Mathematics, University of Houston

ANNUAL REPORT – UNIVERSITY OF HOUSTON

June 24, 2023

Research and education activities (Year 1)

Students: 1 undergraduate student, 3 graduate students and 1 postdoctoral researcher have been involved in Year 1 of the grant.

- ◇ Undergraduate student:
  - Quang Hoang (UH).
- ◇ Graduate Students:
  - Yerbol Palzhanov (UH),
  - Qi Sun (UH),
  - Alexander Zhiliakov (UH).
- ◇ Postdoctoral Researcher:
  - Michele Girfoglio (SISSA).

Zhiliakov participated in two conferences (SIAM TX-LA Section Annual meeting in 2020 and SIAM CSE 2021). Zhiliakov has been offered an Animation Technology Internship at Walt Disney Pictures for Summer 2021.

Research and education activities (Year 2)

Hoang was admitted to the Phd program in Mathematics at Clemson University.

The following **students** have started or continued to be involved in Year 2 of the grant:

- Undergraduate student:
  - Natalia Hajlasz (Harvard),
  - Valeria Vela (Harvard).
- Graduate Students:
  - Yerbol Palzhanov (UH),
  - Qi Sun (UH),
  - Alexander Zhiliakov (UH).
- Postdoctoral Researcher:
  - Michele Girfoglio (SISSA).

Zhiliakov and Sun have graduated in Spring 22. Zhiliakov has accepted a position at Mathworks, while Sun has accepted a post-doc position at UNC (advisor: Boyce Griffith). Palzhanov presented work related to this project at the Finite Element Rodeo 2022. Girfoglio has accepted an assistant professor position at SISSA.

Research and education activities (Year 3)

The following **students** have started or continued to be involved in Year 3 of the grant:

- ◇ Undergraduate student:
  - Nicola Clinco (SISSA).
- ◇ Graduate Students:
  - Lander Besabe (UH),
  - Yerbol Palzhanov (UH).

Clinco has work on his master thesis at SISSA and is about to graduate in Aerospace Engineering at the Politecnico di Torino (Italy). He is considering taking a PhD position at SISSA. Palzhanov presented his work at one conference (SIAM TX-LA Section Annual meeting in 2022). He is expected to graduate in Spring 2024.

Research and education activities (Year 1)

- **Research Presentations:** Quaini presented the research related to this NSF proposal at 5 conferences and seminars: Invited talk at ICERM workshop on Algorithms for Dimension and Complexity Reduction (online, 03/23-27/20), Invited talk at AMS Fall Central Sectional Meeting 2020 (online, 09/12-13/20), Invited talk at World Congress on Computational Mechanics (online, 01/11-15/21), Seminar for the Department of Mathematics at Friedrich-Alexander-Universität Erlangen-Nürnberg (online, 02/01/2021), Invited talk at 2021 SIAM Conference on Computational Science and Engineering (online, 03/01-05/21). Olshanskii presented the research related to this NSF proposal at Comput. Math. and Applications Seminar of Math. Institute, Oxford (Oct. 2020; online); Invited talk at SIAM TX-LA meeting (Oct. 2020; online).

Research and education activities (Year 2)

- **Research Presentations:** Quaini presented the research related to this NSF proposal at 5 conferences and seminars: Fellow's talk at Harvard Radcliffe Institute (Harvard University, 04/12/2022), Invited talk at the Workshop "Calcolo scientifico e modelli matematici", Consiglio Nazionale Delle Ricerche (Rome, 06/6-8/22), Invited talk at the 16th U.S. National Congress on Computational Mechanics (online, 07/25-29/21), Invited talk at the 2021 SIAM Conference on Mathematical and Computational Issues in the Geosciences (online, 06/21-24/21), Keynote talk at IX International Conference on Coupled Problems in Science and Engineering (online, 06/14-16/21).

Research and education activities (Year 2)

- **Research Presentations:** Olshanskii presented the research related to this NSF proposal at 7 conferences and seminars: Invited talk at "A journey in numerical linear algebra: a workshop in honor of Michele Benzi's 60th birthday" (June 2022; University of Pisa), Keynote talk at MS "Advances in numerical methods for inhomogeneous viscous flows: non-Newtonian, viscoelastic, multiphase, eddy-viscosity and other complex models" (June 2022; Eccomas 2022, Oslo), plenary talk at Shanks Workshop on Mathematical Aspects of Fluid Dynamics (Feb. 2022; Vanderbilt University), Colloquium talk at Math. Dept of Texas A&M University (February 2022), Invited talks at 6th Annual SIAM Central States Meeting (Oct. 2021; online), SIAM Southeast meeting (Sept. 2021; Auburn University), Seminar of the DFG Research-Unit 3013: Vector- and Tensor-Valued Surface PDEs (Sept. 2021; online) and Seminar Numerische Mathematik of Weierstrass Institute for Applied Analysis and Stochastics, Berlin (June 2022).

Research and education activities (Year 3)

- **Research Presentations:** Quaini presented the research related to this NSF proposal at 10 conferences and seminars: Seminar talk at the University of Houston (4/28/23), Seminar talk at Virginia Tech (online, 02/02/2023), Colloquium at the Center for Mathematics and Artificial Intelligence, George Mason University (online, 01/27/23), Talk at the 2022 TX-LA Annual Meeting (Houston, 11/04-06/22), Invited talk at SIAM MDS22 (San Diego, 09/26-30/22), Invited talk at AMS Sectional Meetings (University of Texas at El Paso, 09/17-18/22), Colloquium at the University of South Carolina (online, 09/15/22), Invited talk at the 2022 SIAM Annual Meeting (Pittsburgh, 07/11-15/22), Invited talk at the World Congress on Computational Mechanics (online, 07/31-08/05/22), Invited talk at the conference to honor Roland Glowinski (Sorbonne Université, 07/5-8/22).

Research and education activities (Year 3)

- **Research Presentations:** Olshanskii presented the research related to this NSF proposal at 6 conferences and seminars: Keynote talk at AMS special session "Recent Developments in Numerical Methods for PDEs" at Joint Mathematics Meetings (January 2023; Boston, MA); Invited talks at MS "Immersed Boundary Methods for Coupled Problems" at 10th International Conference on Computational Methods for Coupled Problems in Science and Engineering (June 2023; Chania, Greece); MS "'Toward robust and efficient embedded and immersed method for fluid dynamics: stable and very high order formulations" at 22nd IACM Computational Fluids Conference (April 2023; Cannes, France); "Special Session on Modern Trends in Numerical PDEs" at AMS Sectional Meeting (April 2023; Cincinnati, OH); Seminar on Scientific Computing at Clemson University (October 2022; Clemson, SC); "O.A. Ladyzhenskaya centennial conference on PDEs" (online, July 2022)

Research and education activities (Year 1)

- **Courses for graduate and undergraduate students:** In the fall semesters 2020 and spring semester 2021 Quaini has taught Numerical Analysis for graduate students. In the fall semester 2020 Quaini has taught Linear Algebra with Matlab. Topics of this project were mentioned as examples in this course to motivate the students.
- **Organization of Mini-Symposia:** Topics from this project have been or will be presented at the following Mini-Symposia organized by Quaini: "Recent Advances in Scientific Computing and Applications" at AMS Fall Central Sectional Meeting (online, 09/12-13/20), "Advances in Intrusive and Non-intrusive Techniques in Reduced Order Modelling for Flow Analysis, Control and Optimization" at ECCOMAS 2020 (online, 01/11-15/21), "Reduced Order Methods for Parametric CFD Problems" at SIAM CSE (online, 03/01-05/21), "Advances in Coupled Model Reduction in Heat Transfer, CFD and FSI" at COUPLED PROBLEMS 2021 (online, 06/13-16/21), "Model reduction and machine learning for fluids and fluid-structure interactions" at the Mechanistic Machine Learning and Digital Twins for Computational Science, Engineering and Technology (San Diego, 09/23-26/21).

Research and education activities (Year 1, 2, 3)

During Year 2, Quaini has been the 2021-22 William and Flora Hewlett Foundation Fellow at the Radcliffe Institute for Advanced Study, Harvard University. Thus, she had no teaching duties.

- **Organization of Conferences and Workshop** (Year 1, 2, and 3): Quaini is co-chairing with Dr. Rozza (SISSA, Italy) the International Workshop on Reduced Order Methods, to be held at the National University of Singapore during 05/22-26/23.
- **Organization of Mini-Symposia** (Year 2): Topics from this project will be presented at the following Mini-Symposia organized by Quaini: "Recent trends in Model Order Reduction for coupled problems" at the X International Conference on Computational Methods for Coupled Problems (Crete, 06/5-7/23). "Recent Advances in Scientific Computing and Applications" at the AMS Fall Central Sectional Meeting (UTEP, 09/17-18/2022), "Advances in intrusive and non-intrusive order reduction techniques for flow analysis, control and optimization" at the 15^{th} World Congress on Computational Mechanics (online, 07/31-08/05/22).

Research and education activities (Year 3)

During Year 3, Quaini has had teaching relief in the fall due to childbirth.

- **Course for graduate and undergraduate students:** In spring 2023 Quaini has taught Advanced Linear Algebra. Topics of this project were mentioned as examples in this course to motivate the students.
- **Organization of Conferences and Workshop** (Year 3): Quaini and Olshanskii were organizers of the 5th Annual Meeting of the SIAM TX-LA Section.
- **Organization of Mini-Symposia** (Year 3): Topics from this project will be presented at the following Mini-Symposia organized by Quaini: "Recent trends in Model Order Reduction for coupled problems" at the X International Conference on Computational Methods for Coupled Problems (Crete, 06/5-7/23); "Modeling, analysis and numerical simulations involving thin structures" at the Annual Meeting of the SIAM TX-LA Section (University of Houston, 11/4-6/22); and co-organized by Olshanskii: "Immersed Boundary Methods for Coupled Problems" MS at X International Conference on Computational Methods for Coupled Problems (Crete, 06/5-7/23); "Modeling, analysis and numerical simulations involving thin structures" the SIAM TX-LA Section (Houston, 11/4-6/22); "Numerical models with free boundaries and interfaces" MS at

Motivation

Liposomes (typical diameter <100 nm) are lipid vesicles with a bilayered membrane structure.

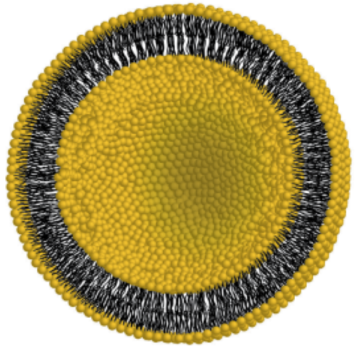

Liposomes are considered to be the most successful drug carriers.

Despite extensive research, only a few liposomal drugs have been approved by the U.S. Food and Drug Administration.

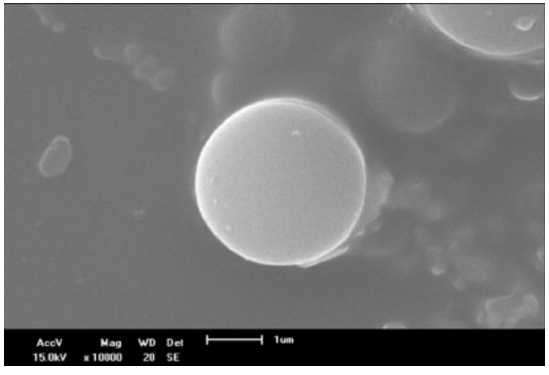

Key liposomal characteristics are

- high target selectivity
- enhanced target cell uptake
- limited toxicity

A promising class of liposomes

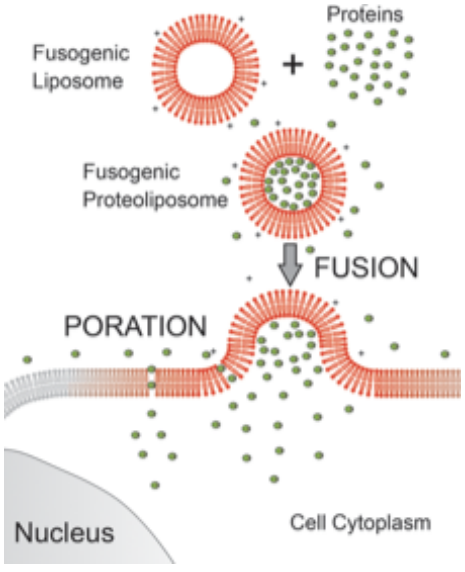

Fusogenic liposomes are liposomes formulated to facilitate fusion.

Membrane fusion provides a neat strategy for delivery of therapeutic molecules across the cellular plasma membrane into the cell interior.

Fusogenic liposomes successfully deliver biomolecules into cells. However, the fusion-inducing components needed for efficient delivery make these liposomes toxic in vivo.

One needs to find a balance between fusogenicity and toxicity.

Possible solution: low concentrations of fusogenic lipids that can be presented in dense patches through phase separation.

Our goal: to apply complementary mathematical, computational, and experimental tools to design and develop a new class of liposomal carriers, called patchy fusogenic liposomes.

Lateral phase separation with conservation

Conservation law for representative concentration c on stationary $\Gamma \subset \mathbb{R}^3$:

$$\rho \frac{\partial c}{\partial t} + \operatorname{div}_\Gamma \mathbf{j} = 0$$

ρ: total density of the system

$\mathbf{j} = -M \nabla_\Gamma \mu$: diffusion flux (Fick's law, empirical)

$M = M(c)$: mobility coefficient

$\mu = \frac{\delta f}{\delta c}$: chemical potential

$f(c) = f_0(c) + \frac{1}{2}\epsilon^2 |\nabla_\Gamma c|^2$: total specific free energy (Ginzburg-Landau potential)

In order to have phase separation, f_0 must be a non-convex function of c.

Surface Cahn–Hilliard equation

$$\rho \frac{\partial c}{\partial t} - \operatorname{div}_\Gamma \left(M \nabla_\Gamma \left(f_0' - \epsilon^2 \Delta_\Gamma c \right) \right) = 0 \quad \text{on } \Gamma$$

TraceFEM: basic principles

We study for the first time a geometrically unfitted finite element method for the Cahn–Hilliard equation

2D illustration

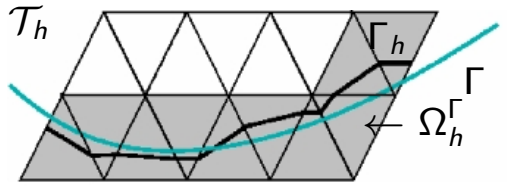

Idea

Use a trace space induced by FE functions for the bulk triangulation $\mathcal{T}_h$.

Define

Define the outer space: $V_h = \{v \in C(\Omega_h^\Gamma) : v \in \mathbb{P}_1(T) \text{ for any } T \in \mathcal{T}_h^\Gamma\}$

And then define the trace space for V_h:

$$\text{interface FE space } V_h^\Gamma := \{\psi_h \in C(\Gamma_h) : \exists\, v_h \in V_h : \psi_h = v_h|_{\Gamma_h}\}.$$

Qualitative comparison with experiments

Two-component mixture with random initial condition (1:1), $\epsilon = 0.01$ (realistic value)

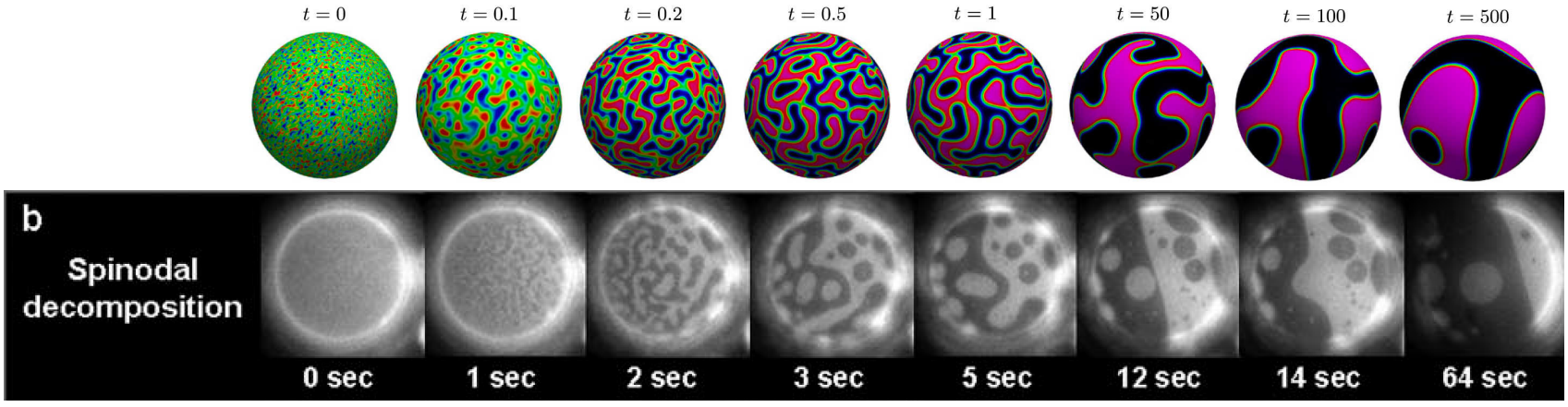

Two-component mixture with random initial condition (2:1), $\epsilon = 0.01$

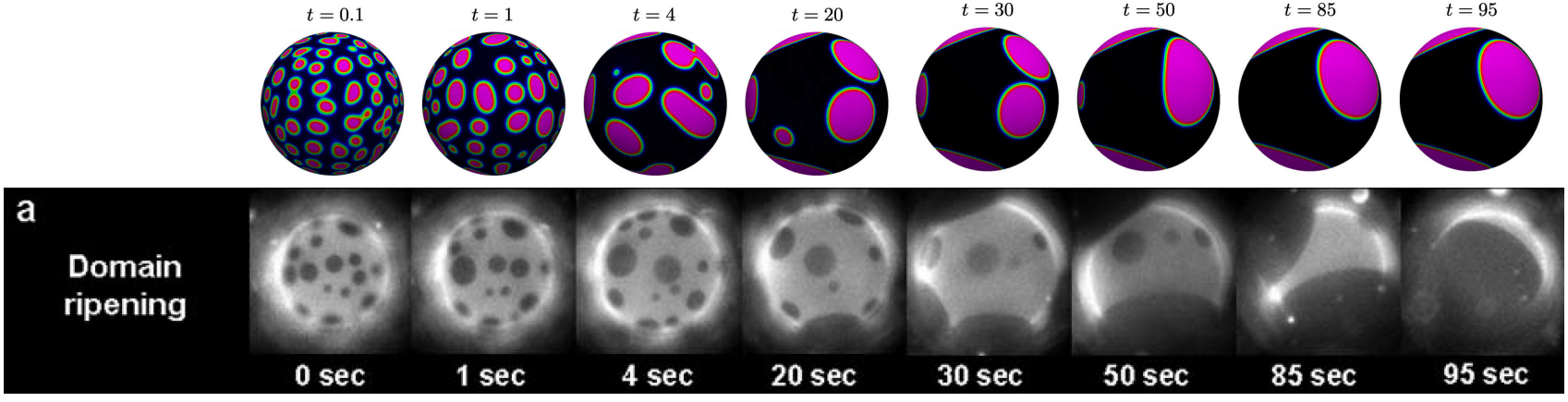

Advantages of TraceFEM

- Surface Γ is not meshed directly.
- Number of active degrees of freedom is optimal, it is comparable to methods in which Γ is meshed directly.
- Optimal order of convergence in L^2 norms.
- Amenable to both space and time adaptivity.
- Effective condition numbers of matrices are comparable to common FEMs.
- If Γ evolves, Γ is not tracked by a mesh (Eulerian method).
- If Γ evolves, one recomputes matrices using the same data structures.

Lateral phase separation on an evolving surface

Using elementary tangential calculus, we derive a Cahn–Hilliard problem posed on an evolving material surface:

$$\dot{\rho} + \rho \mathrm{div}_\Gamma \mathbf{u} = 0 \quad \text{on } \Gamma(t)$$

$$\dot{c} - \rho^{-1} \mathrm{div}_\Gamma \left(M \nabla_\Gamma \left(\frac{1}{\epsilon} f_0' - \epsilon \Delta_\Gamma c \right) \right) = 0 \quad \text{on } \Gamma(t)$$

where $\dot{f}$ is the material derivative of f.

- The system is one-way coupled
- We are not aware of a minimization property for the Cahn–Hilliard problem in time-dependent domains $\rightarrow$ the system is no longer dissipative

Evolving surface: weak formulation

To be able to use an Eulerian approach, we introduce an arbitrary smooth extension of c and μ to a neighborhood

$$\mathcal{O}_\delta(\Gamma(t)) = \{\mathbf{x} \in \mathbb{R}^3 \,:\, \mathrm{dist}(\mathbf{x}, \Gamma(t)) < \delta\}.$$

and reformulate the problem in terms of the extended variables.

The weak formulation becomes:

$$\int_{\Gamma(t)} \rho \left(\frac{\partial c}{\partial t} + \mathbf{u} \cdot \nabla c \right) v \, ds + \int_{\Gamma(t)} M \nabla_\Gamma \mu \, \nabla_\Gamma v \, ds = 0,$$

$$\int_{\Gamma(t)} \mu \, q \, ds - \frac{1}{\epsilon} \int_{\Gamma(t)} f_0'(c) \, q \, ds - \epsilon \int_{\Gamma(t)} \nabla_\Gamma c \, \nabla_\Gamma q \, ds = 0,$$

$$\frac{\partial \mu}{\partial \mathbf{n}} = \frac{\partial c}{\partial \mathbf{n}} = 0 \quad \text{in } \mathcal{O}_\delta(\Gamma(t)),$$

for all smooth v and q defined in $\Gamma(t)$.

We discretize first in time (semi-implicit Euler method) and then apply TraceFEM for space discretization. Everything else is like the stationary surface case presented in [Yushutin-Q.-Majd-Olshanskii, *IJNMBE* 2019]

Simple motion

We consider the following synthetic solutions

$$c^* = \frac{1}{2}\left(x_1 x_2 + 1\right), \quad t \in [0, 0.1]$$

on a unit sphere that is translated and rotated, with $\epsilon = 0.1$, $h_\ell = \frac{10/3}{2^{\ell+2}}$, $\Delta t = 4^{1-\ell}/10$.

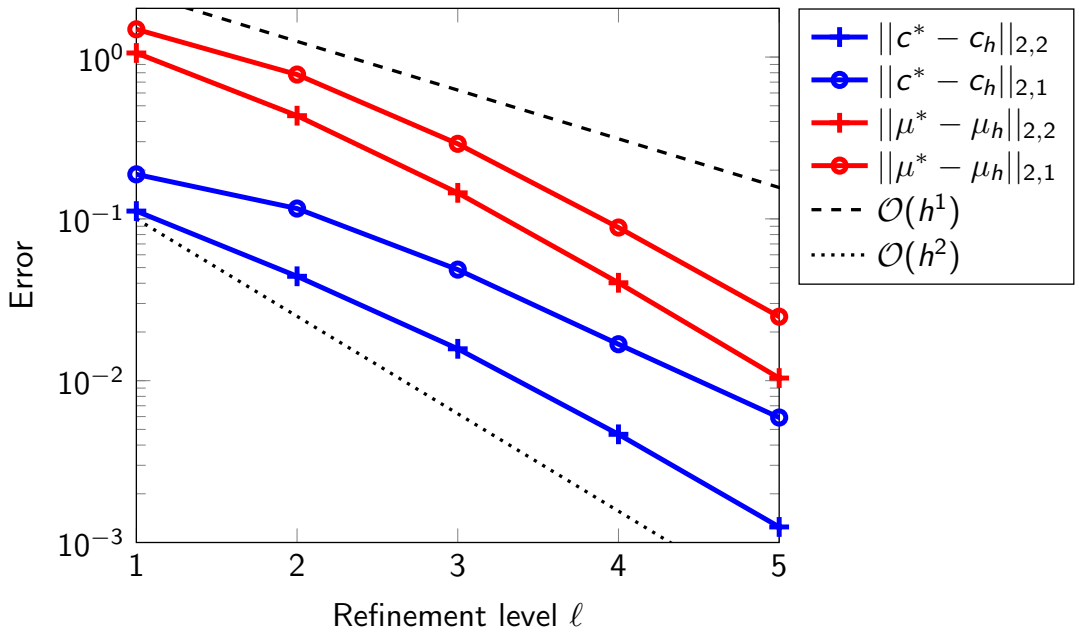

Oscillating ellipsoid

We consider time-dependent surface $\Gamma(t)$ to be an oscillating ellipsoid. As initial solution, we take:

$$c_0 = 0.5 + 0.05\cos(2\pi x_1)\cos(2\pi x_2)\cos(2\pi x_3).$$

We set $\epsilon = 0.01$, $h_\ell = \frac{10/3}{2^{\ell+2}}$, $\Delta t = 0.01$.

Discrete Lyapunov energy:

$$E_h^L(c_h) = \int_{\Gamma_h} f(c_h) ds$$

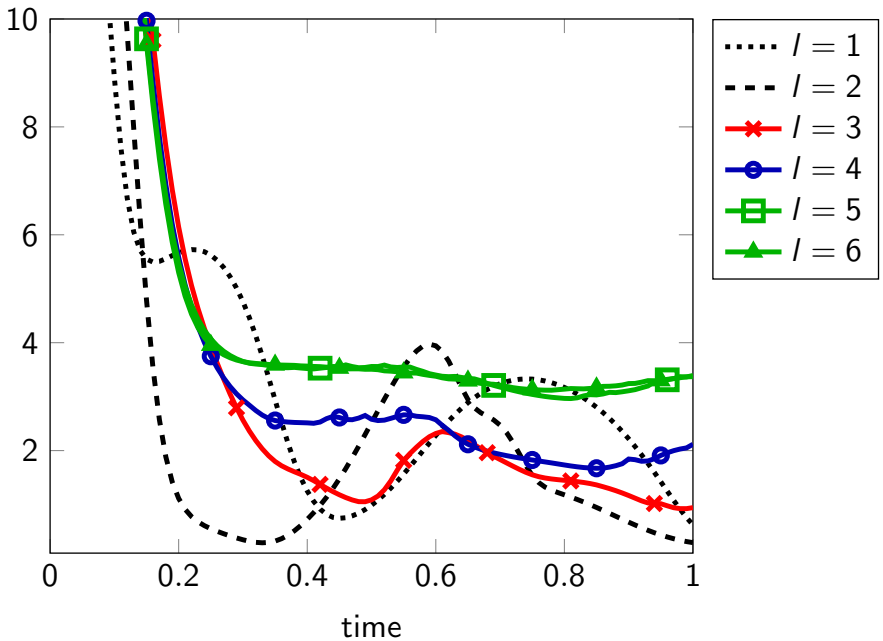

Colliding spheres with pre-separated phases

The evolving surface is the zero level set of level set function

$$\phi(\mathbf{x}, t) = 1 - \frac{1}{||\mathbf{x} - \mathbf{x}_c^+(t)||^3} - \frac{1}{||\mathbf{x} - \mathbf{x}_c^-(t)||^3},$$

with

$$\mathbf{x}_c^{\pm}(t) = \pm \left(\frac{3}{2} - t, 0, 0 \right), \quad t \in [0, 1.5].$$

We take an initial solution with pre-separated phases on each ball.

$t = 0.23$ $t = 0.25$ $t = 1$

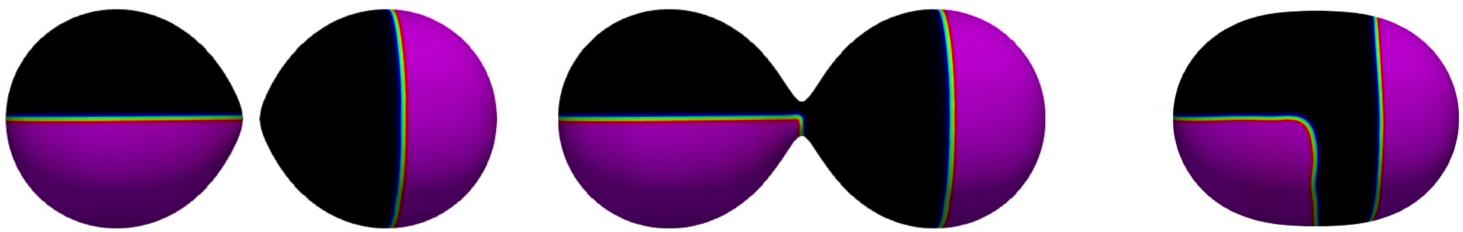

Pattern formation on colliding spheres

Same surface dynamics as before, but different initial condition:

- two-component mixture with random initial condition (1:1) for the ball initially centered at $\mathbf{x}_c^-(0)$
- homogeneous phase for the ball initially centered at $\mathbf{x}_c^+(0)$

We set $\epsilon = 0.01$.

Slow collision

$t = 0.23$ $t = 0.26$ $t = 1.23$

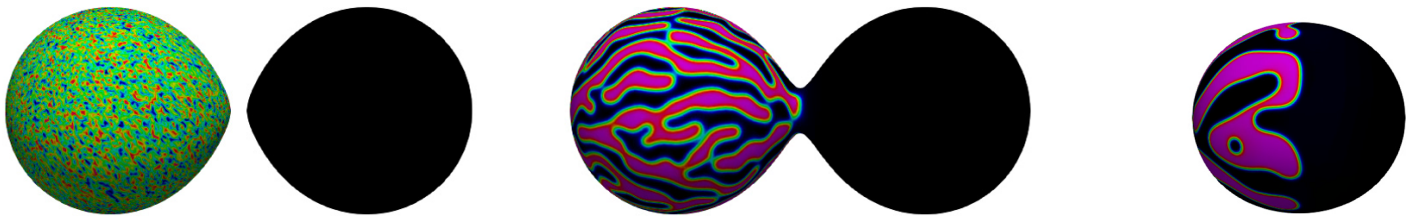

Fast collision

$t = 0.023$ $t = 0.025$ $t = 0.123$

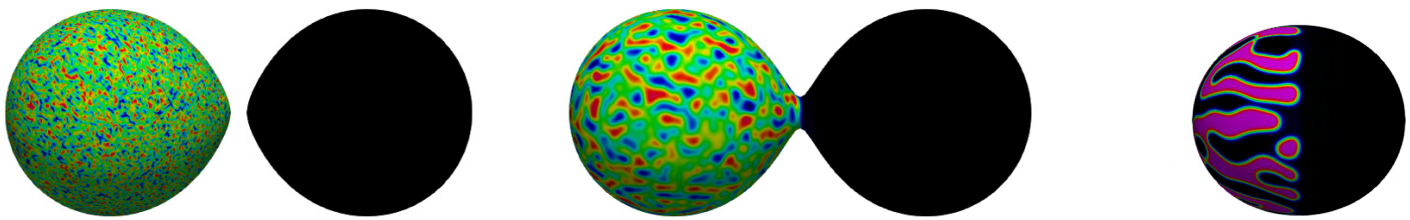

One paper reporting on these results has been published in in the Journal of Computational Physics in 2020.

Comparison with Majd's experiments

We compared the numerical results produced by our geometrically unfitted solver for the Cahn–Hilliard model on steady surfaces with experiments conducted in Majd's lad for two membrane compositions:

- DOPC:DPPC with a 3:1 molar ratio with 20% Cholesterol (referred to as 3:1:20%), yielding $9(\pm\ 1.1)\%$ lipid domain area fraction.
- DOPC:DPPC with a 2:1 molar ratio with 20% Cholesterol (referred to as 2:1:20%), yielding $15.7(\pm\ 1.5)\%$ lipid domain area fraction.

To set the initial state for numerical simulations, we relied on thermodynamic considerations.

For both compositions, we performed:

- a qualitative comparison between numerical results and epi-fluorescence microscopy images.
- a quantitative comparison total lipid domain perimeter over time and total number of lipid domains over time.

The results are reported in a paper appeared in BBA - Biomembranes in 2021.

Qualitative comparison for composition 3:1:20%

Epi-fluorescence microscopy images (with black background) and numerical results (with white background) at four different times in time interval $[194, 800]$ s.

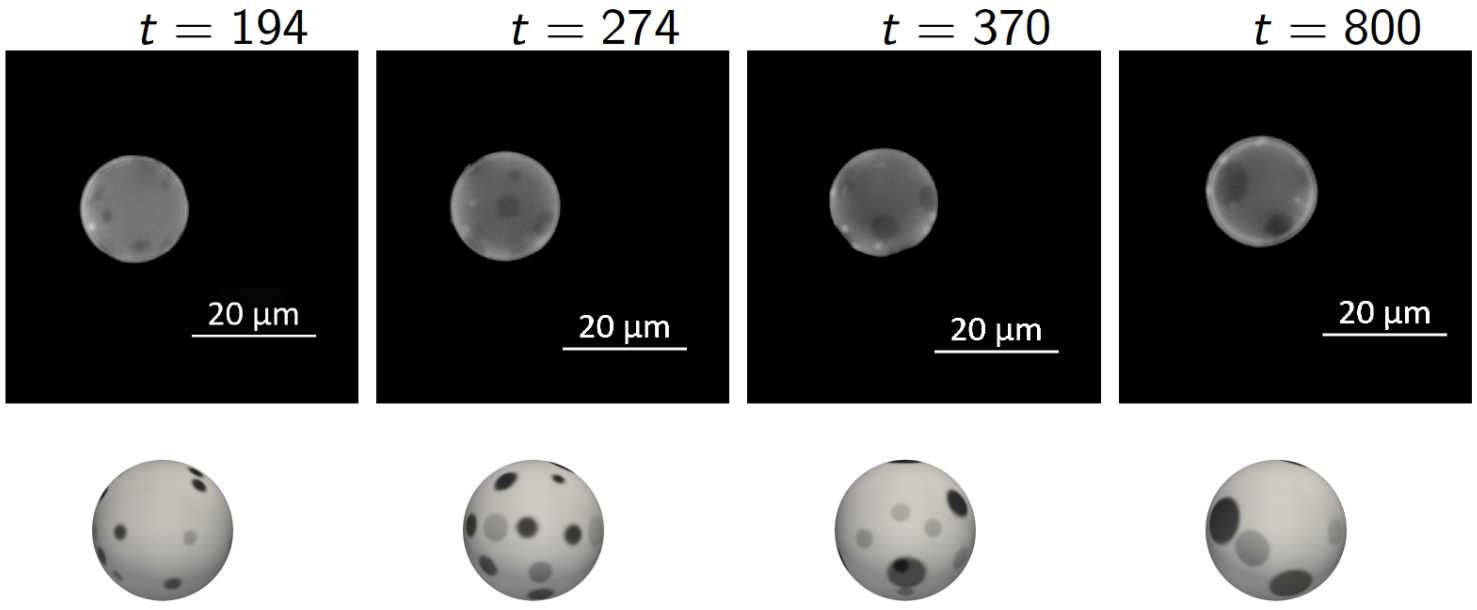

Click any picture above to run the full animation of a representative simulation.

Qualitative comparison for composition 2:1:20%

Epi-fluorescence microscopy images (with black background) and numerical results (with white background) at four different times in time interval $[124, 294]$ s

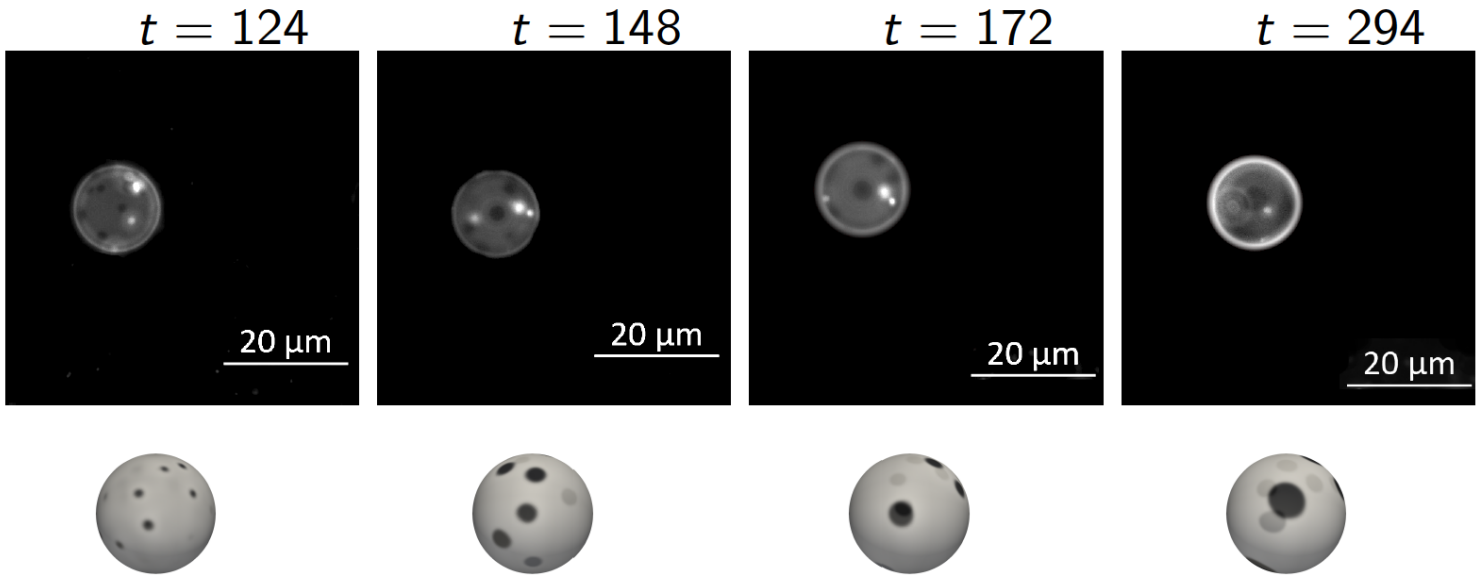

Click any picture above to run the full animation of a representative simulation.

Quantitative comparison with Majd's experiments

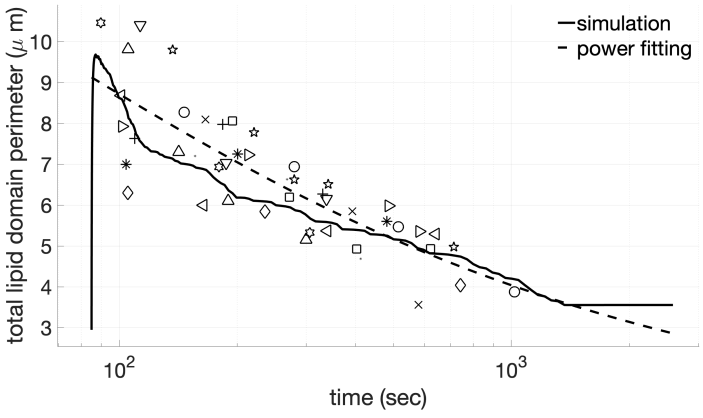

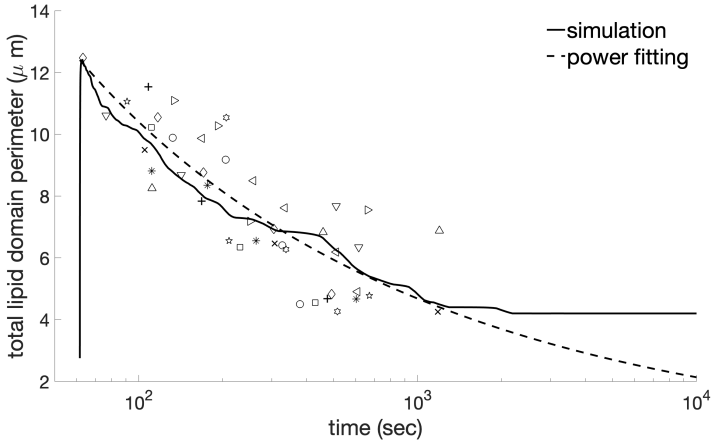

Left: Total lipid domain perimeter over time for composition 3:1:20%: numerical results average (solid line), power curve fitting (dashed line), experimental data (markers). Right: Total lipid domain perimeter over time for composition 2:1:20%: numerical results average (solid line), power curve fitting (dashed line), experimental data (markers).

Quantitative comparison with Majd's experiments

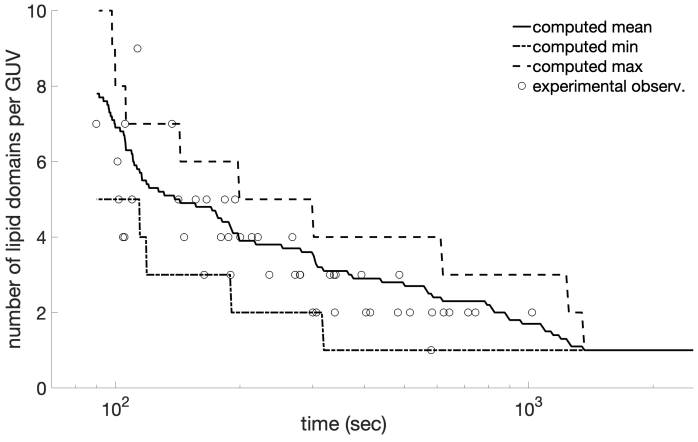

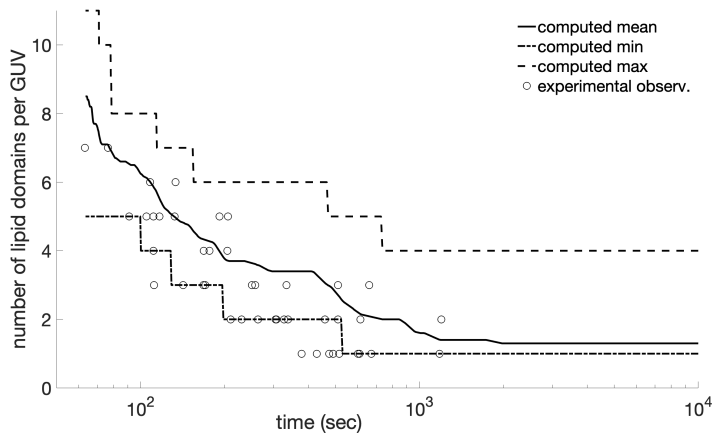

Total number of lipid domains over time for composition 3:1:20% (left) and 2:1:20% (right): numerical results average (solid line), minimal and maximum values found numerically (dash-dotted and dashed lines, respectively), and experimental data (circles).

In conclusion, our computational approach delivers not only qualitative pictures, but also accurate quantitative information about the dynamics of the membrane organization.

Navier–Stokes–Cahn–Hilliard system

While the results produced by the Cahn–Hilliard model agree well with the considered experimental data, they do not capture the viscous and fluidic phenomena present in lipid vesicles. Thus, we proposed a more complex thermodynamically consistent phase-field model.

$$\rho\partial_t\mathbf{u}+\rho(\nabla_\Gamma\mathbf{u})\mathbf{u}-\mathbf{P}\mathrm{div}_\Gamma(2\eta E_s(\mathbf{u}))+\nabla_\Gamma p=-\sigma_\gamma c\nabla_\Gamma\mu+M\theta(\nabla_\Gamma(\theta\mathbf{u}))\nabla_\Gamma\mu+\mathbf{f},$$

$$\mathrm{div}_\Gamma\mathbf{u}=0,$$

$$\partial_t c+\mathrm{div}_\Gamma(c\mathbf{u})-\mathrm{div}_\Gamma(M\nabla_\Gamma\mu)=0,$$

$$\mu=\tfrac{1}{\epsilon}f_0'-\epsilon\Delta_\Gamma c.$$

- η: dynamic viscosity of the mixture
- $\mathbf{u}$: surface averaged tangential velocity
- $E_s(\mathbf{u})$: surface rate-of-strain tensor
- σ_γ: line tension
- p: fluid pressure
- $\theta^2 = \frac{d\rho}{dc}$

Thanks to the term in red, the model allows for a non-linear dependence of fluid density on the phase-field order parameter.

Navier–Stokes–Cahn–Hilliard (NSCH) system

We apply an unfitted finite element method (TraceFEM) to discretize the system and introduce a fully discrete time-stepping scheme with the following properties:

1. the scheme decouples the fluid and phase-field equation solvers at each time step;
2. the resulting two algebraic systems are linear;
3. the numerical solution satisfies the same stability bound as the solution of the original system under some restrictions on the discretization parameters.

One paper on the NSCH model and the proposed unfitted finite element methodology has appeared in Computer Methods in Applied Mechanics and Engineering in 2021.

Kelvin–Helmholtz instability on a sphere

With the proposed method we could study the effect of line tension on the surface Kelvin–Helmholtz instability, a well-known two-phase fluid flow.

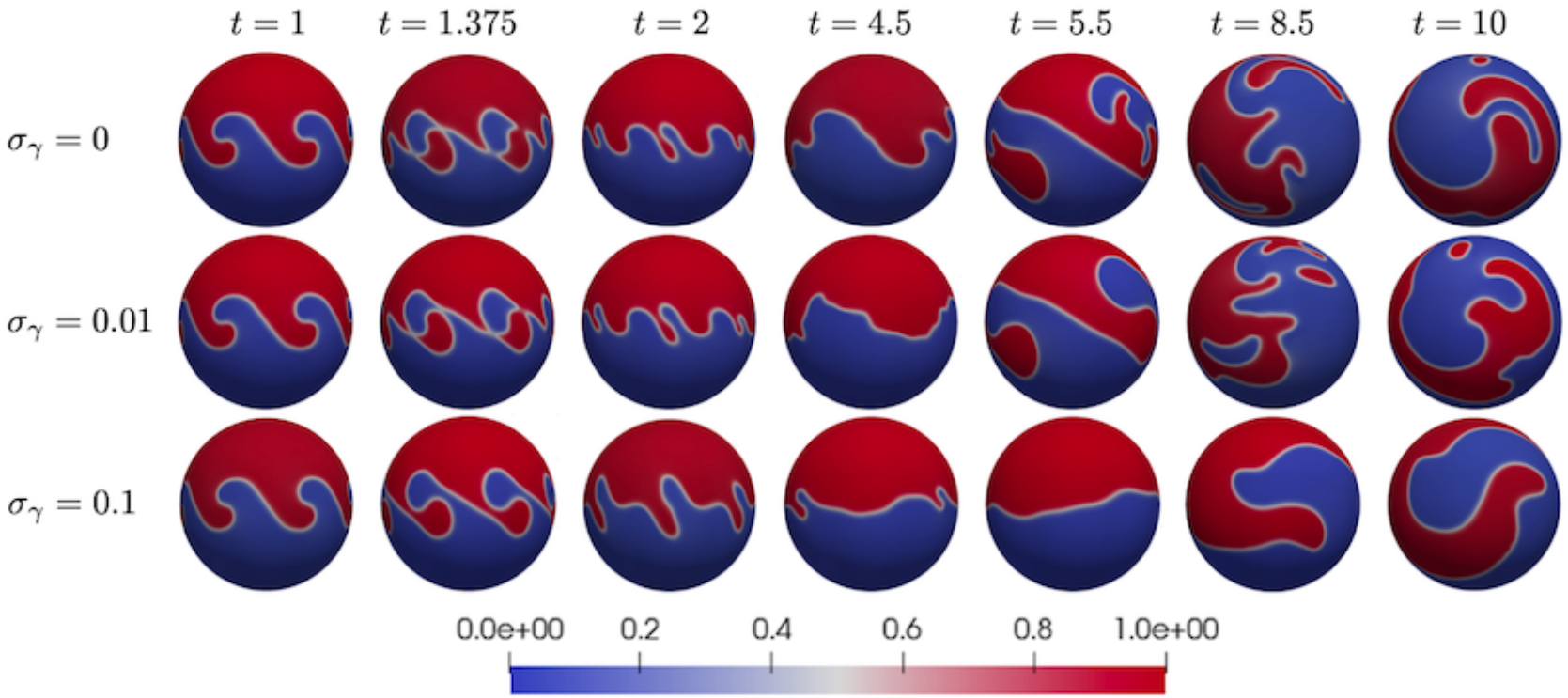

Evolution of order parameter for different values of line tension: $\sigma_\gamma = 0$ (top), $\sigma_\gamma = 0.01$ (center), and $\sigma_\gamma = 0.1$ (bottom). A full animation can be viewed following the link youtu.be/C3_WLO1Wd7Y

Kelvin–Helmholtz instability on a sphere

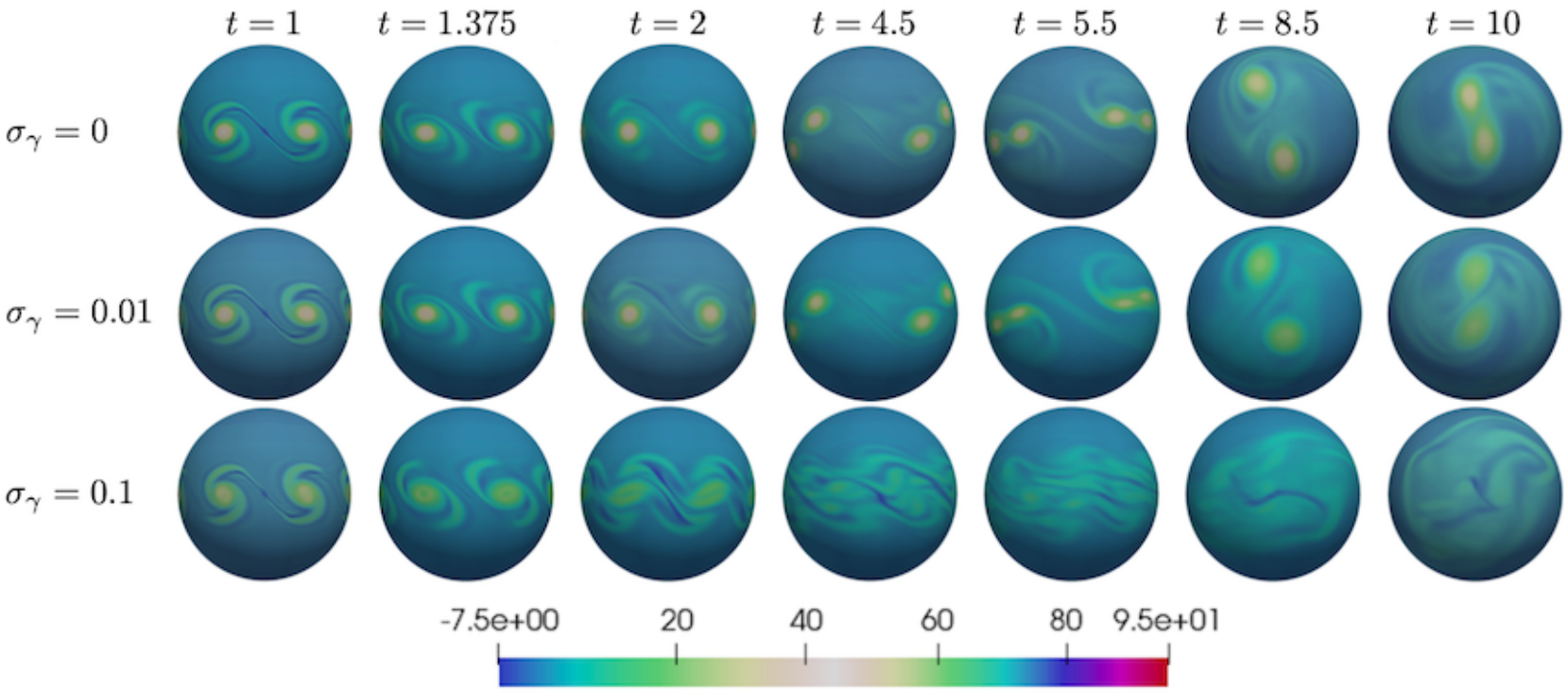

Evolution of the vorticity for different values of line tension: $\sigma_\gamma = 0$ (top), $\sigma_\gamma = 0.01$ (center), and $\sigma_\gamma = 0.1$ (bottom). A full animation can be viewed following the link youtu.be/FdMznBuMJPE

Rayleigh–Taylor instability on a torus

Another well-known two-phase fluid flow is the Rayleigh–Taylor instability. With the proposed method we could study the effect of viscosity and surface shape on the surface Rayleigh–Taylor instability.

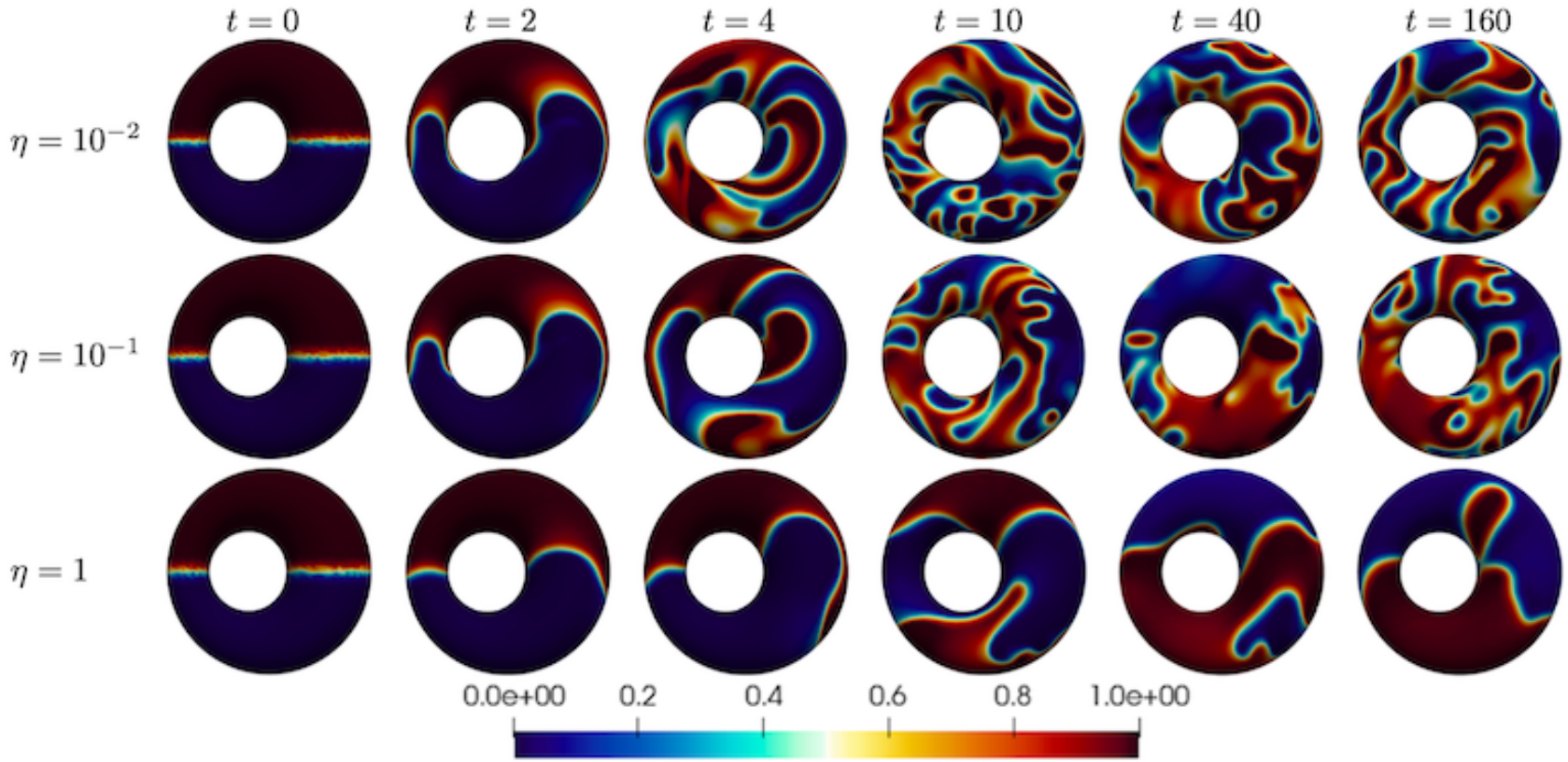

Evolution of the order parameter for $\sigma_\gamma = 0.025$ and different values of viscosity: $\eta = 10^{-2}$ (top), $\eta = 10^{-1}$ (center), and $\eta = 1$ (bottom). A full animation can be viewed following the link youtu.be/FTqqFjvzEZg

Comparison with Majd's experiments

We compared the results obtained with the NSCH model on steady surfaces with data provided by Majd for two membrane compositions:

- DOPC:DPPC with a 1:2 molar ratio with 25% Cholesterol, yielding about 70% liquid ordered area fraction.
- DOPC:DPPC with a 1:1 molar ratio with 15% Cholesterol, yielding about 30% liquid ordered area fraction.

These compositions yield opposite and nearly inverse phase behavior. The CH model would predict nearly the same evolution of the domain ripening process for these two compositions.

For both compositions, we performed again:

- a qualitative comparison between numerical results and epi-fluorescence microscopy images.
- a quantitative comparison total lipid domain perimeter over time and total number of lipid domains over time.

The results are reported in a paper appeared in BBA - Biomembranes in 2022.

Qualitative comparison with Majd's experiments

- Composition yielding about 70% liquid ordered area fraction. (Click for video)

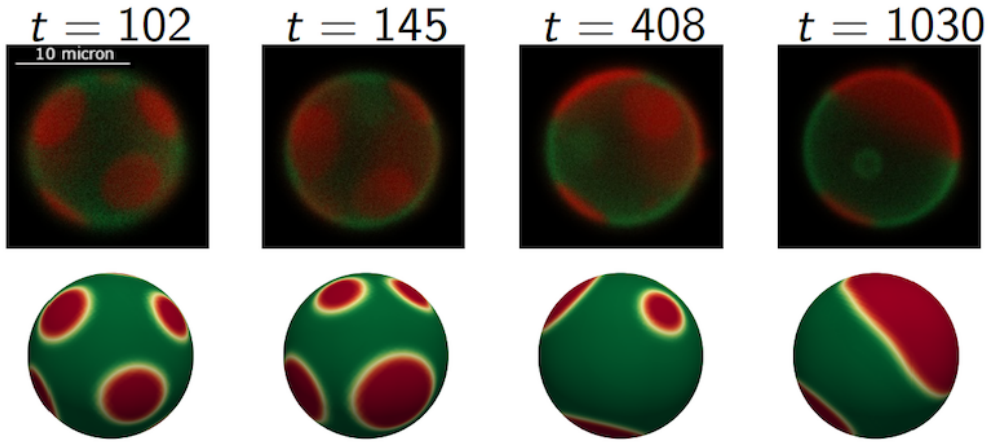

- Composition yielding about 30% liquid ordered area fraction. (Click for video)

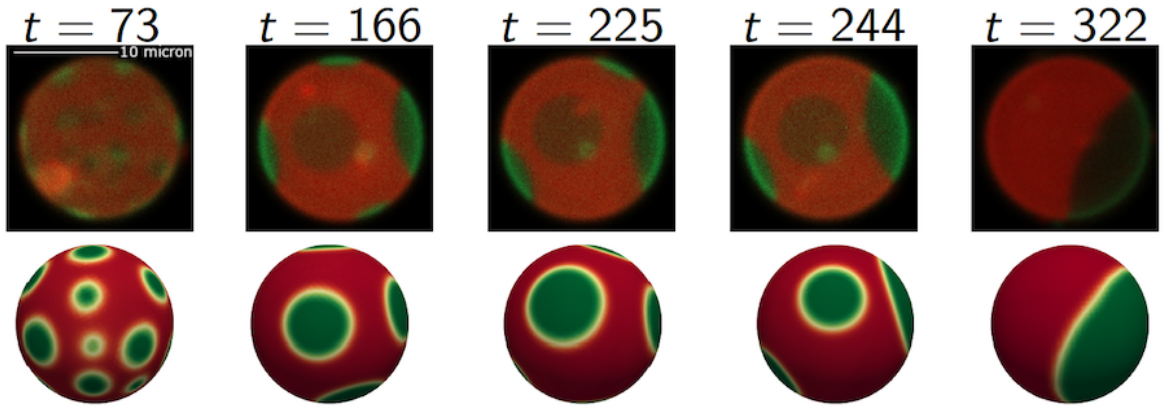

Green: liquid ordered phase. Red: liquid disordered phase.

Quantitative comparison with Majd's experiments

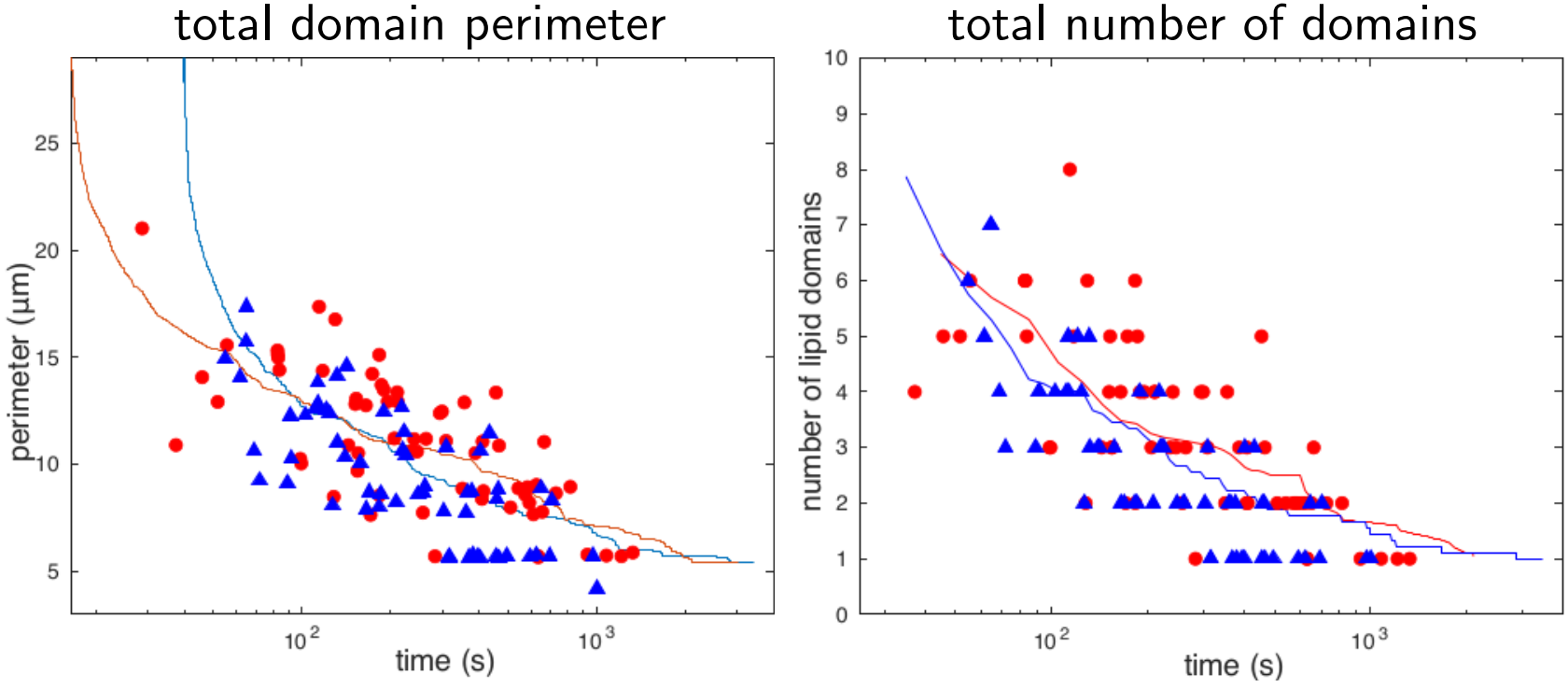

Red dots: experimental data for 70% liquid ordered area fraction.
Red line: computed mean for 70% liquid ordered area fraction.
Blue triangles: experimental data for 30% liquid ordered area fraction.
Blue line: computed mean for 30% liquid ordered area fraction.

Note that the NSCH model can reproduce the differences in the coarsening dynamics for these two compositions that the CH model cannot capture.

Further comparison with Majd's experiments

For the case of 70% liquid ordered area fraction, lab experiments revealed a **metastable phase**, possibly due to the formation of some temporary molecular complexes. In fact, besides vesicles with red patches on green background (see p. 30, top), vesicles with green patches on red background were observed (left).

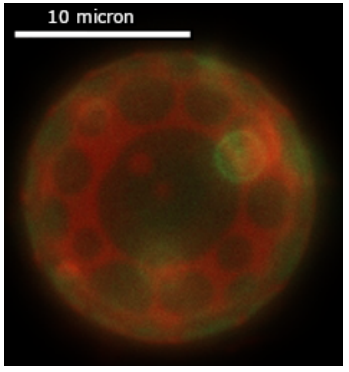

Interestingly, such rare patterns were not observed in our numerical simulations. However, with an ad-hoc initial condition, we managed to emulate the metastable phase with the NSCH model. (Click for video)

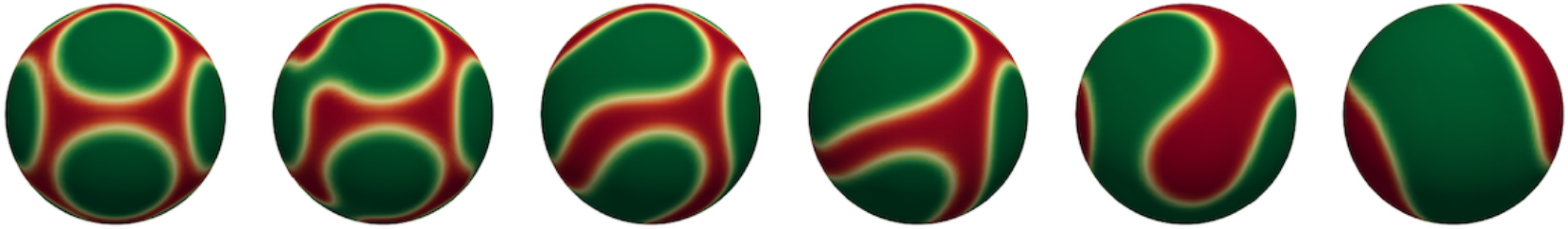

The comparisons between numerical and experimental data are reported in a paper appeared in BBA - Biomembranes in 2022.

CH model vs NSCH model

Since for the simulation of lateral phase separation and coarsening in lipid membranes we have used phase-field models with lateral flow (i.e., the NSCH model) and without lateral flow (i.e., the CH model), we ran a computational study to investigate the effect of the presence of lateral flow on the evolution of phases. In particular, we focused on understanding how variable line tension, viscosity, membrane composition, and surface shape affect the pattern formation. For all the cases under consideration, we computed the discrete Lyapunov energy (defined at p. 17) and observed the evolution of phases.
We observed that the discrete Lyapunov energy decays faster when using the NSCH model. In particular, such faster decay is more significant when the line tension is increased and the viscosity is lowered. The latter is more evident in some membrane compositions (i.e., 70% liquid ordered area fraction) than others (i.e., 50% liquid ordered area fraction). Finally, by comparing the evolution of phases on the sphere and on the torus we do observe differences that indicate an effect of the surface geometry.

This study is presented in a paper appeared in the Vietnam Journal of Mathematics in 2022. Representative results are reported next.

CH vs NSCH: comparison of Lyapunov energy decay

sphere, 50% l_o, variable viscosity

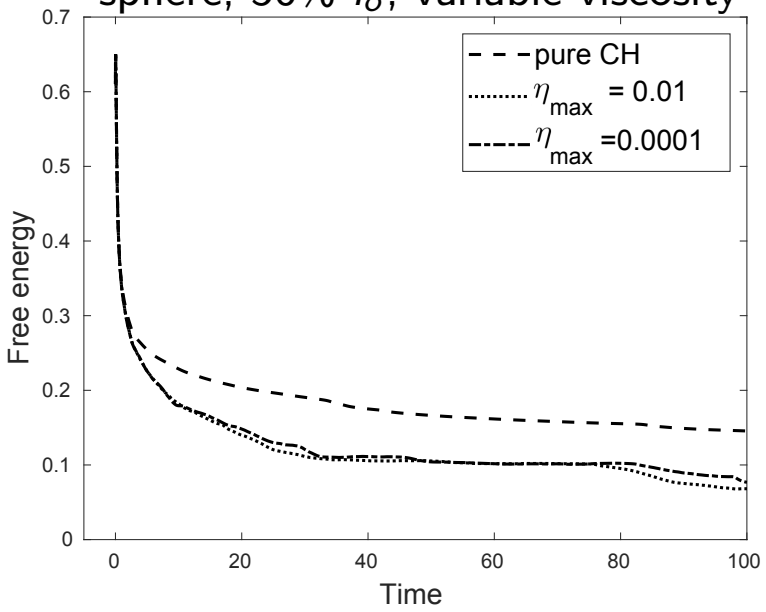

sphere, 70% l_o, variable viscosity

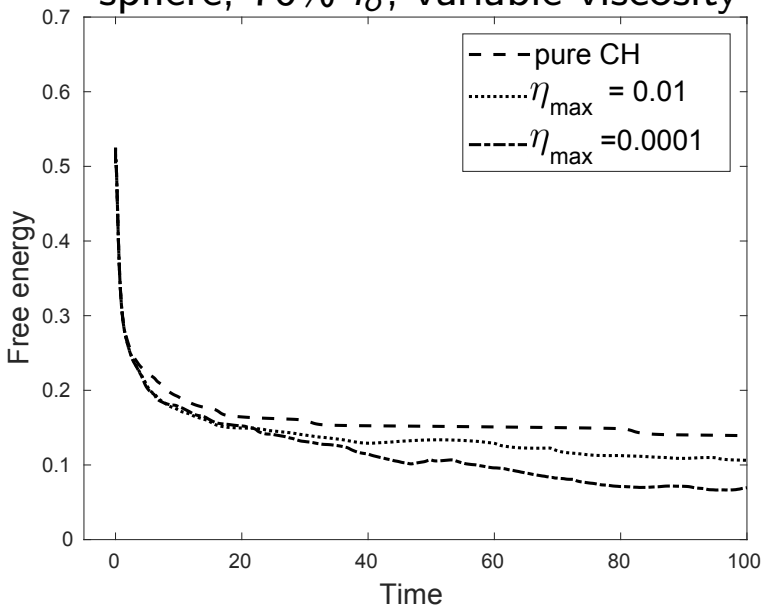

torus, 50% l_o, variable viscosity

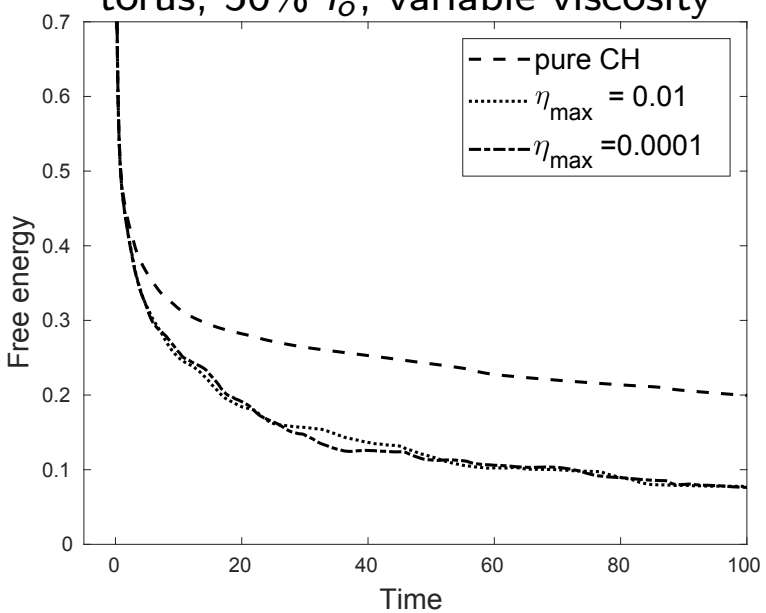

sphere, 50% l_o, variable line tension

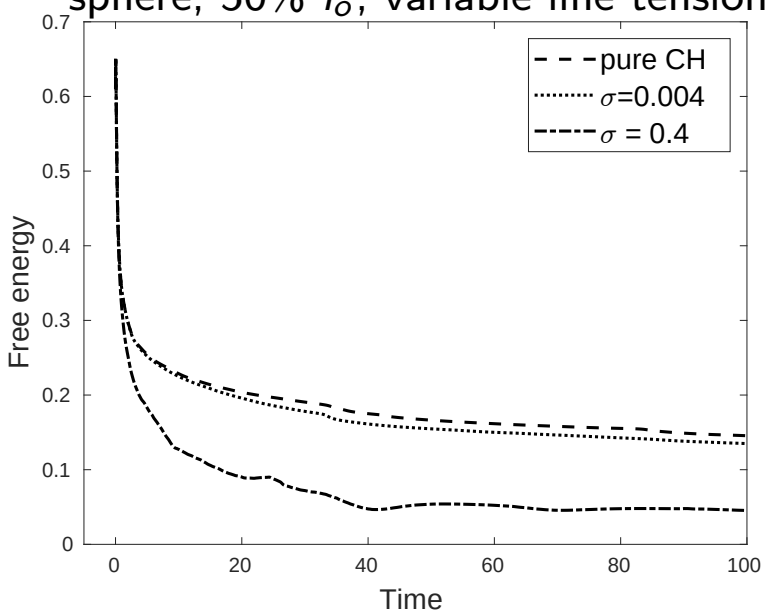

CH vs NSCH: evolution of phases

Case: sphere, 50% l_o area fraction, variable viscosity.

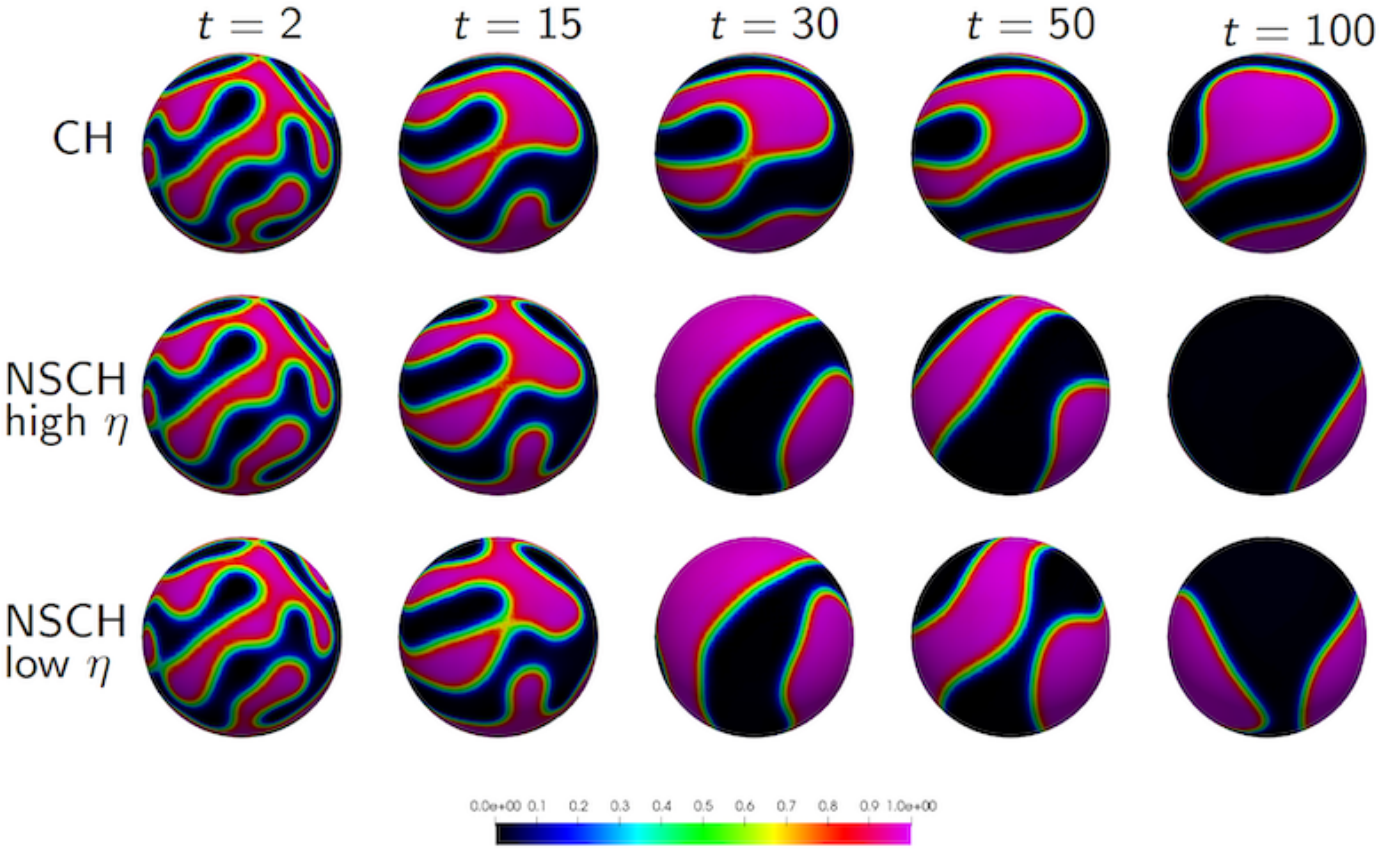

Switching from high viscosities to low viscosities in the NSCH model does not produce significant differences in the appearance of the domains until $t = 100$ for this composition. Compare center and bottom row.

CH vs NSCH: evolution of phases

Case: sphere, 70% l_o area fraction, variable viscosity.

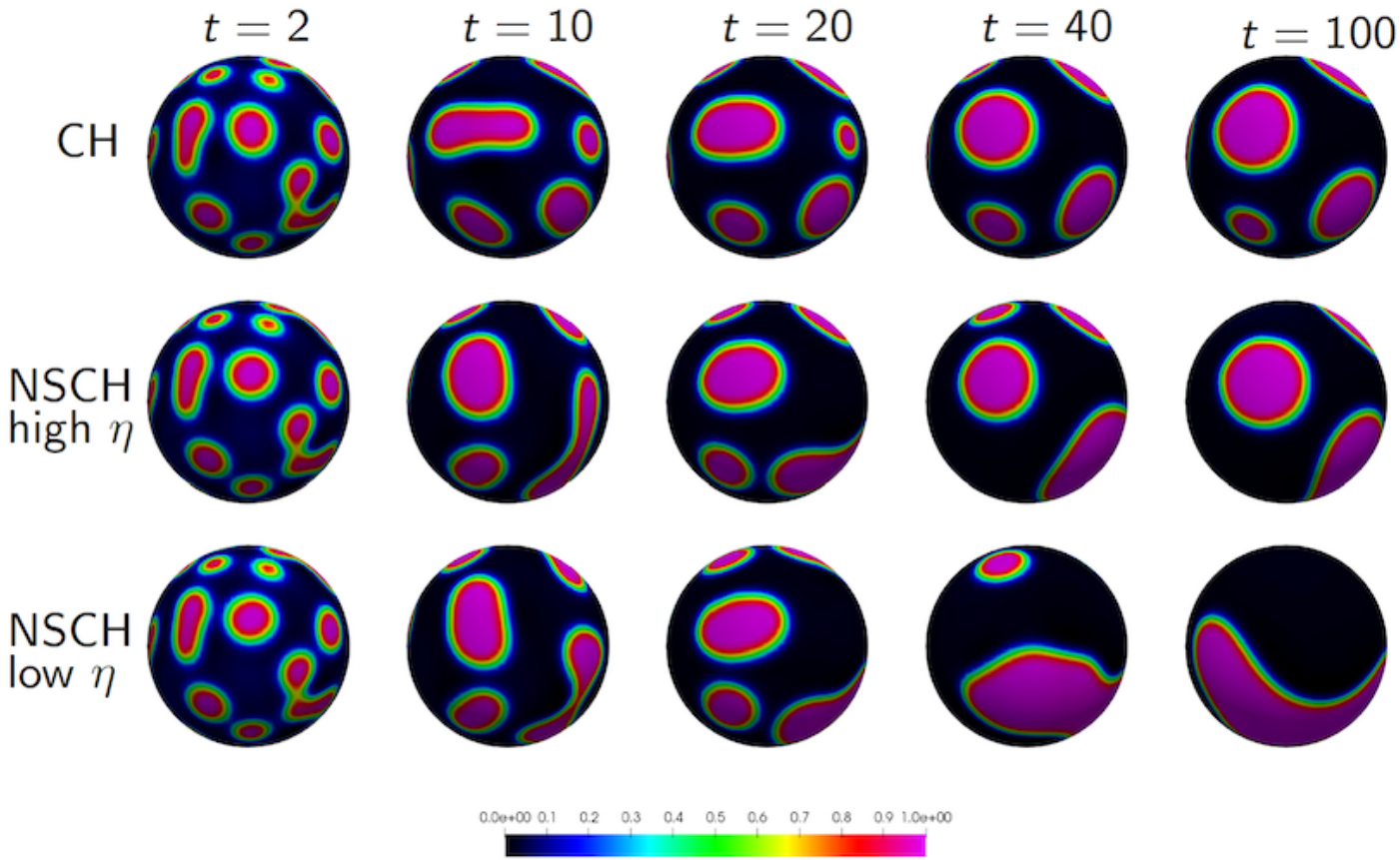

The patterns are very different from the previous composition. The change in domain appearance happens faster when going from high viscosities to low viscosities for this composition. Indeed, by comparing center and bottom row we observe remarkable differences at $t = 40$.

CH vs NSCH: evolution of phases

Case: torus, 50% l_o area fraction, variable viscosity.

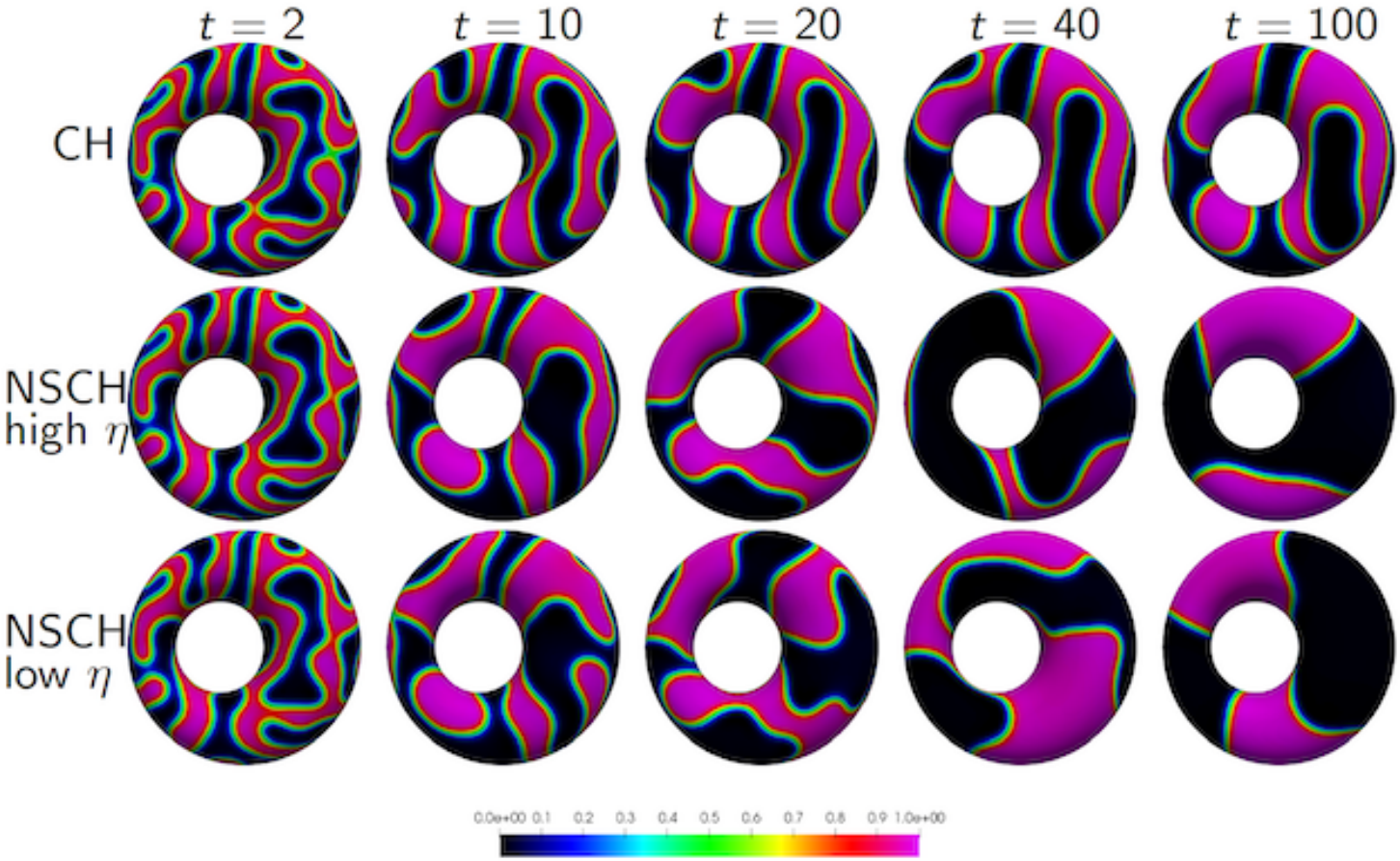

We see that the interface separating the two phases remains tortuous for a longer period of time on the torus when compared to the sphere. As within the torus itself, we do not observe a particular difference in pattern between "skinny" and "fat" side of the torus.

Fast Algebraic Solver for surface fluid model

We proposed a preconditioner for the algebraic system of the surface Navier-Stokes problem. Our approach is based on the augmentation of the matrix (as in the Augmented Lagrangian approach), cheap Schur complement preconditioners and factorization of velocity blocks and recycling of factors over several time steps in the FGMRES as a solver.

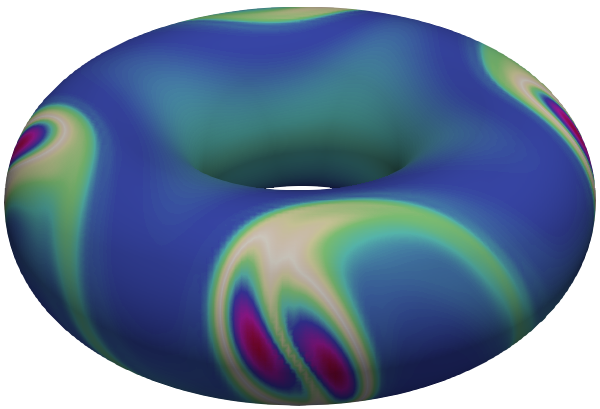

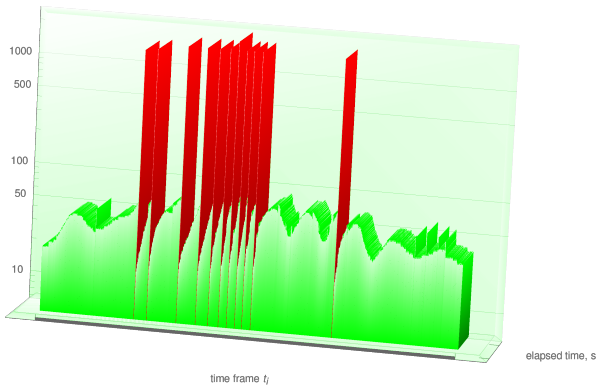

Kelvin-Helmholz vorticies on torus is an example of a high Re number flow computed thanks to the now available algebraic solver. Complexity of solver on every time step is illustrated on the right histogram.

The solver was found to be robust with respect to Re number, nearly optimal w.r.t. #d.o.f. and computationally fast. Analysis includes mesh independent spectral bounds. A paper joint with a PhD student was published in Numerical Linear Algebra with Applications.

SAV method for the surface CH model

The scalar auxiliary variable (SAV) method allows to construct efficient and accurate time discretization schemes for a large class of gradient flows. Since its introduction, SAV methods have been developed for various applications, which include epitaxial thin film growth models, models for one- and multi-component Bose-Einstein condensates, and square phase field crystal model.
We applied the SAV method to the surface CH problem and proved that the CH problem with the scalar auxiliary variable is energy stable when discretized in space by TraceFEM and in time by either BDF1 or BDF2. In addition, we proposed adaptive time stepping schemes for increased efficiency. We compared the numerical results obtained with the SAV method against the results obtained with a stabilized scheme inspired from [Shen-Yang, *Discrete & Continuous Dynamical Systems* 2010] and presented in [Yushutin-Quaini-Majd-Olshanskii, *IJNMBE* 2019].

A paper on this work is in preparation. We expect to have it ready for submission in the next two months. Representative results are reported next.

SAV method: convergence test

We consider the following exact solution:

$$c^*(t,\mathbf{x}) = \frac{1}{2}\left(1+\tanh\frac{x_3}{2\sqrt{2}\epsilon}\right), \quad t\in[0,1],$$

on a unit sphere with $\epsilon = 1, 0.1, 0.05$, $h_\ell = \frac{10/3}{2^{\ell+1}}$, and time step refinement.

The table below reports the L_2 errors of c at $t = 1$ computed with the SAV method, $\mathbb{P}^1$ elements, and BDF2 for different mesh levels ℓ and time steps, together with the rates of convergence.

		$\epsilon = 0.05$		$\epsilon = 0.1$		$\epsilon = 1$	
ℓ	Δt	error	rate	error	rate	error	rate
3	0.02	$2.8338\cdot10^{-2}$		$1.3438\cdot10^{-2}$		$0.3474\cdot10^{-2}$	
4	0.01	$0.9727\cdot10^{-2}$	1.54	$0.3824\cdot10^{-2}$	1.81	$0.0767\cdot10^{-2}$	2.18
5	0.005	$0.2869\cdot10^{-2}$	1.76	$0.1013\cdot10^{-2}$	1.91	$0.0181\cdot10^{-2}$	2.07
6	0.0025	$0.0732\cdot10^{-2}$	1.96	$0.0255\cdot10^{-2}$	1.98	$0.0045\cdot10^{-2}$	2.01

We observe optimal convergence. We have highlighted in red the digits that are different from the errors obtained with the stabilized method from [Yushutin-Quaini-Majd-Olshanskii, IJNMBE 2019].

SAV method: phase separation

Further comparison between the SAV method and the stabilized method from [Yushutin-Quaini-Majd-Olshanskii, IJNMBE 2019] for:

- Composition yielding about 50% liquid ordered area fraction.

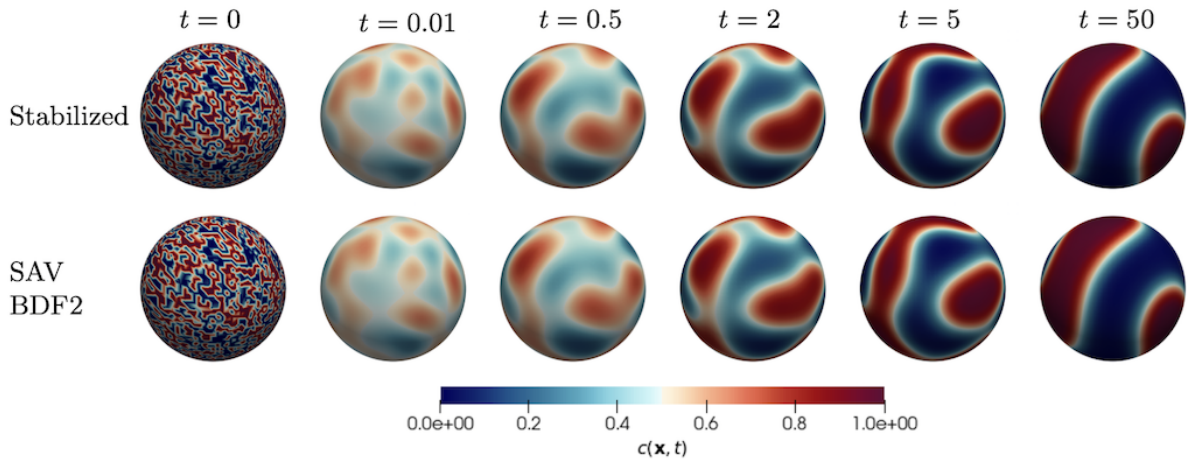

- Composition yielding about 30% liquid ordered area fraction.

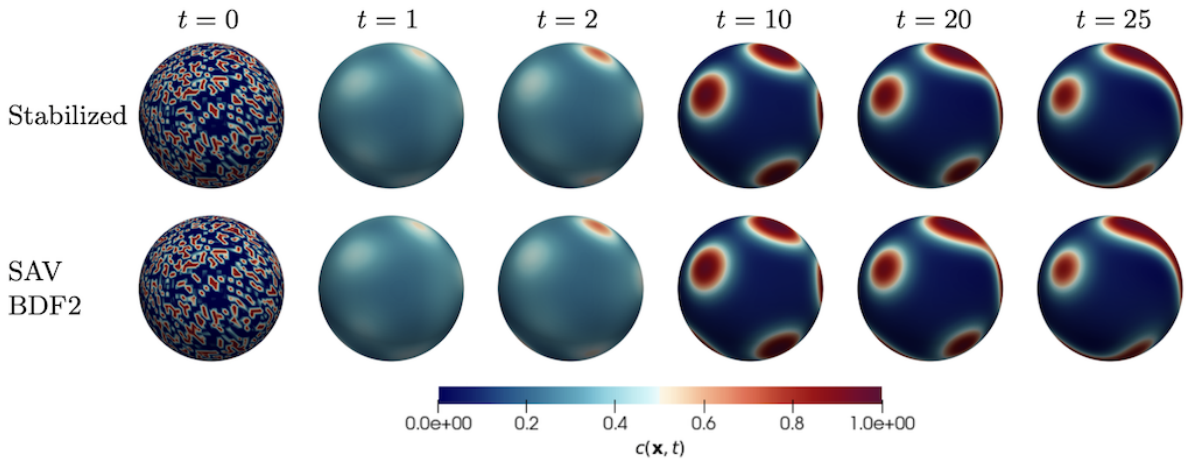

Phase separation with fusogenic lipids

DOPC is replaced with fusion-inducing lipid DOTAP that has a cationic (i.e., positive charge) headgroup but its acyl chain chemistry is similar to DOPC. DOTAP goes primarily to the liquid disordered l_d phase. We considered 3 lipid membrane compositions:

Label	Composition	Lo area fraction	DOTAP% in Ld (DOTAP% in total)	DOTAP in Lo (DOTAP% in total)
PAT1	DOPC: DPPC: Chol=3:1:20%	10.8% (15C)	16.5% (15%)	5.5% (15%)
PAT2	DOPC: DPPC: Chol= 1:1:15%	34.47% (17.5C)	22.6% (15%)	4.56% (15%)
PAT3	DOPC: DPPC: Chol=1:2:25%	70.37% (15C)	40.8% (15%)	8.04% (15%)

The liposomes are created and undergo phase separation (or not in the case of homogeneous liposomes used for comparison) before they are exposed to the model membranes with negative charges, which mimic cells. Ten minutes after such exposure, through microscopy images we are able to tell the percentage of liposomes that have fused with the model membranes.

A paper on this work is in preparation. Representative results are reported next.

Phase separation with fusogenic lipids

Experimental evidence shows that liposomes with composition PAT3 (see table in the previous slide) and 15% total DOTAP have a fusion percentage comparable with homogeneous liposomes that have double positive charge, i.e., 30% total DOTAP.

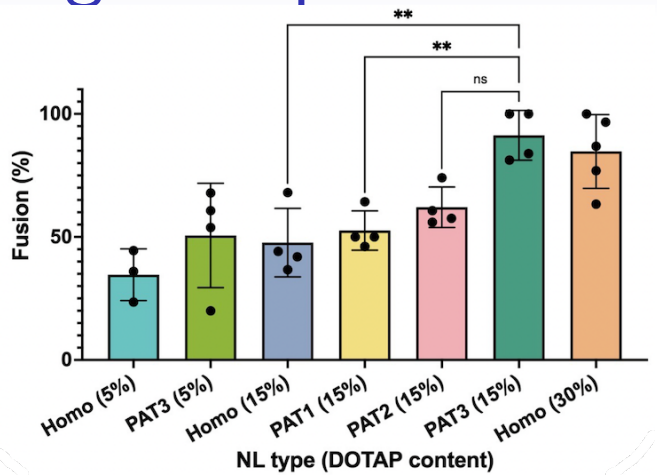

Given the relative size of the liposomes (< 100 nm) and the model membranes ($\approx$10 micron), this phenomenon cannot be explained in terms of electrostatic force alone. It results from the interplay of forces driving phase separation, forces driving surface flow, and electrostatic forces.

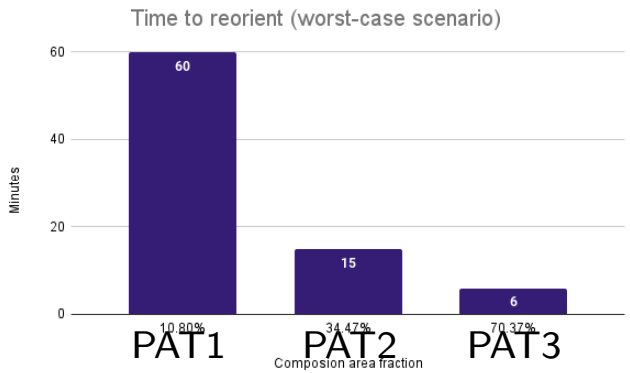

We ran simulations of the phase-separated liposomes exposed to the model membrane in the worst case scenario (i.e., charged domain opposite to the model membrane) and recorded the time needed for the charged domain to face the model membrane.

Such time is minimal in the case of PAT3, which means that the charged patches reorient faster, hence facilitating attraction and then fusion with the model membrane.

Equilibrium states of fluid–elastic membranes

We studied the equilibrium configurations of inextensible *elastic* membranes that exhibit lateral fluidity such as cell membranes. Using a continuum description of the membrane's motions based on the surface Navier–Stokes equations with bending forces, we derived differential equations governing the mechanical equilibrium. The equilibrium conditions are found to be independent of lateral viscosity and relate tension, pressure, and tangential velocity of the fluid. A shape equation is derived that extends the classical Helfrich model with an area constraint to membranes of non-negligible mass. Additionally, we introduced a simple numerical method to compute solutions of the shape equation. Numerical experiments conducted reveal a diverse family of new equilibrium configurations.

The figure on the right shows several equilibrium configurations of fluid membranes of non-negligible area mass. The work was reported in a paper published on arXiv with a revised version currently under review in Physics of Fluids.

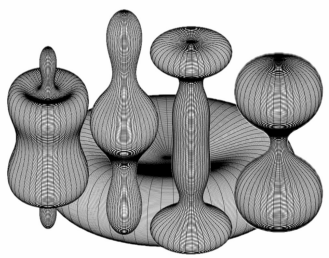

Open-source library

All the computational results presented so far have been performed with open-source software DROPS:

`http://www.igpm.rwth-aachen.de/DROPS/`

An important outcome of this work is that the code created for it will be incorporated in DROPS as an open source resource available to the scientific and the engineering community.

Two-phase Stokes problems with slip between phases

Liposomes encapsulate drugs and are injected into the blood stream to reach their target. Thus, liposomes interact with fluid around and within them. As a first step towards modeling this complex interaction, we worked on two-phase Stokes problems with slip between phases. The two phases would represent the fluid inside and outside the liposome, which have different physical parameters.
For the two-phase Stokes problems we proposed an isoparametric unfitted finite element approach of the CutFEM or Nitsche-XFEM family. In particular, for a class of unfitted finite elements

- we showed an inf-sup stability property with a stability constant that is independent of the viscosity ratio, slip coefficient, position of the interface with respect to the background mesh and, of course, mesh size;
- we proved stability and optimal error estimates that follow from this inf-sup property;
- we provided numerical results in two and three dimensions to corroborate the theoretical findings and demonstrated the robustness of our approach.

3D two-phase Stokes problem with exact solution

We considered a spherical interface between the two phases and the exact solution depicted in the figure below. Let Ω^+ be the domain outside the sphere and Ω^- the domain inside the sphere.

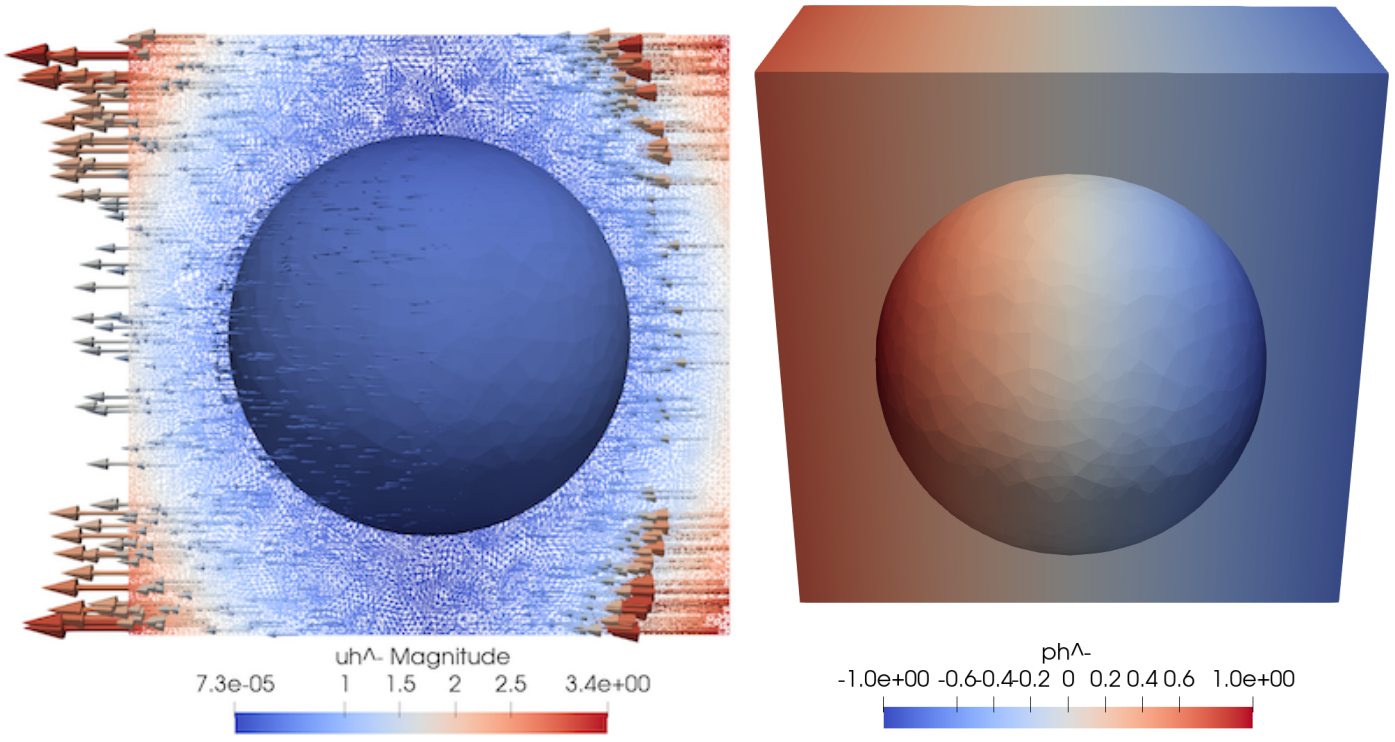

Velocity vectors colored with the velocity magnitude on the *xz*-section of Ω^+ and in Ω^- (left) and pressure in Ω^- and half Ω^+ (right).

3D two-phase Stokes problem with exact solution

We considered structured meshes of tetrahedra with four levels of refinement. The initial triangulation has mesh size $h = 1$ and all the other meshes are obtained by halving h till $h = 0.125$. We chose to use finite element pair $\mathbf{P}_2 - P_1$. Below, we show the L^2 error and a weighted H^1 error for the velocity and a weighted L^2 error for the pressure against the mesh size h

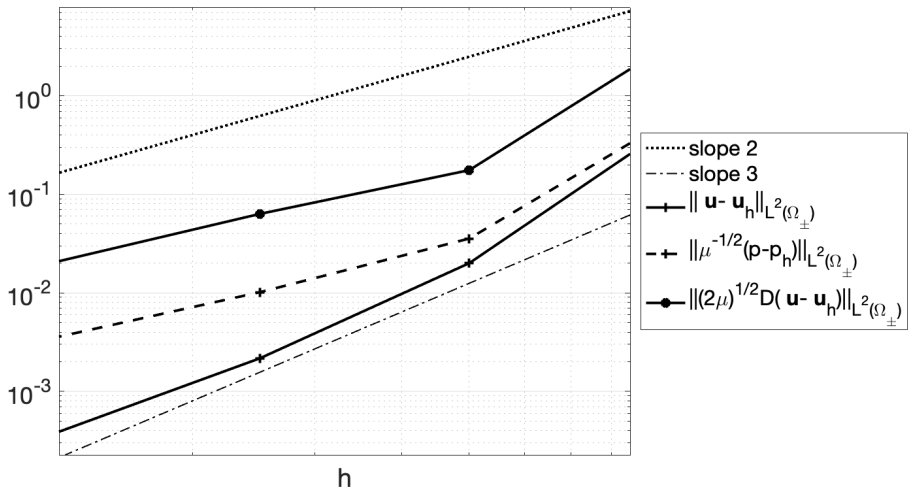

We observe almost cubic convergence in the L^2 norm for the velocity, quadratic convergence in the weighted L^2 norm for the pressure and in the weighted H^1 norm for the velocity.

One paper with these results has appeared in the Journal of Scientific Computing in 2021.

Coupling bulk and surface fluid flows

As a starting point, we considered a simplified version the coupled bulk and surface flow problem: we assumed the system has reached a steady state and inertia terms can be neglected.

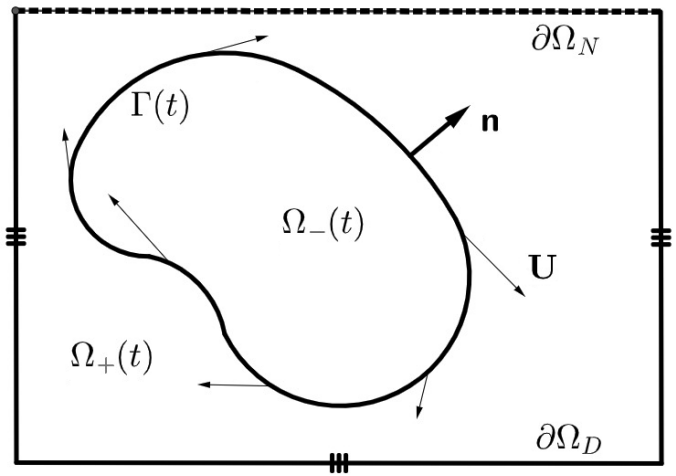

Bulk flow in $\Omega_\pm$:

$$-\mu^\pm \Delta \mathbf{u}^\pm + \nabla p = \mathbf{f}^\pm,$$
$$\nabla \cdot \mathbf{u}^\pm = 0.$$

Surface flow on Γ:

$$-2\mu_\Gamma \mathbf{P}\mathrm{div}_\Gamma \mathbf{D}_\Gamma(\mathbf{U}_T) + \nabla_\Gamma \pi = [\mathbf{P}\boldsymbol{\sigma}\mathbf{n}]^+_-,$$
$$\mathrm{div}_\Gamma \mathbf{U}_T = 0.$$

Coupling conditions

The bulk and surface fluid are coupled by

- the tangential load exerted by the bulk fluid onto the surface fluid (see previous slide);
- balance of the normal component of the normal stresses:

$$[\mathbf{n}^T \boldsymbol{\sigma} \mathbf{n}]_+^- = \pi\kappa \qquad \text{on } \Gamma;$$

- the immiscibility condition:

$$\mathbf{u}^+ \cdot \mathbf{n} = \mathbf{u}^- \cdot \mathbf{n} \qquad \text{on } \Gamma;$$

- slip with friction between the bulk fluid and the viscous membrane:

$$\begin{aligned} \mathbf{P}\boldsymbol{\sigma}^+\mathbf{n} &= f^+(\mathbf{P}\mathbf{u}^+ - \mathbf{U}_T) && \text{on } \Gamma, \\ \mathbf{P}\boldsymbol{\sigma}^-\mathbf{n} &= -f^-(\mathbf{P}\mathbf{u}^- - \mathbf{U}_T) && \text{on } \Gamma. \end{aligned}$$

Coupling bulk and surface fluid flows

For this coupled problem:

- We proved well-posedness.
- We proposed a partitioned strategy for its numerical solution, i.e. bulk and surface flows are solved separately and the coupling conditions enforced in an iterative fashion. The closest domain decomposition approach to the decoupling scheme we proposed is the Robin-Neumann method.
- We provided numerical results in three dimensions to demonstrated the robustness of our approach.

One paper on this work has appeared in Computational Methods in Applied Mathematics 2022.

Exact solution for the coupled problem

We considered an exact solution for a spherical interface between the two phases. To check the spatial accuracy of our scheme, we used structured meshes of tetrahedra with five levels of refinement, the coarsest mesh having mesh size $h = 0.5$ while the finest mesh has $h = 0.05$. We chose finite element pair $\mathbf{P}_2 - P_1$ for both the bulk and surface fluid problems. Below we report the convergence test (left) and the number of bulk-surface iterations of the partitioned method as h varies (right).

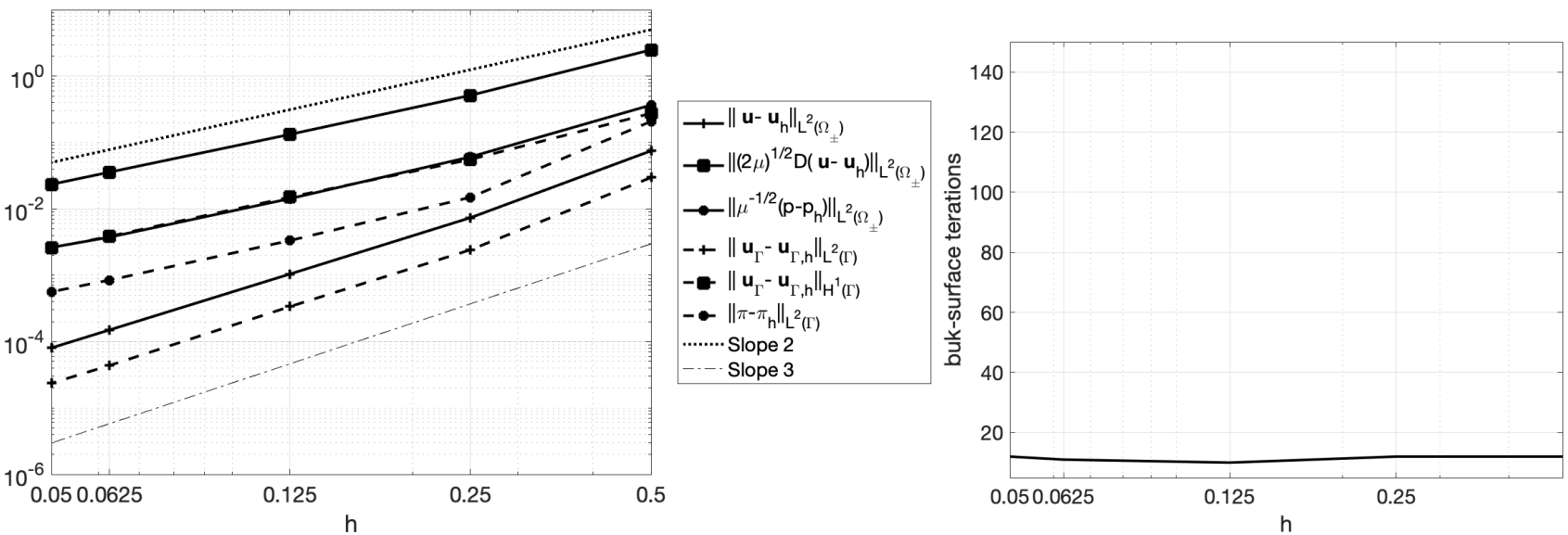

We observe optimal convergence rates for all the norms under consideration. Moreover, the number of iterations is fairly insensitive to a mesh refinement or coarsening.

Open-source library

All the computational results for the two-phase Stokes flow and coupled bulk-surface flow have been obtained with NGsolve:

`https://ngsolve.org/`

a high performance multiphysics finite element software with a Python interface, and add-on library ngsxfem[1], which enables the use of unfitted finite element technologies.

Just like in the case of DROPS, we will incorporate the code created for this project into ngsxfem as a way to give back to the scientific community.

[1] `https://github.com/ngsxfem/ngsxfem/tree/49205a1ae637771a0ed56d4993ce99008f3a00e0`

Reduced order models

We introduced a reduced order model (ROM) for numerical integration of a dynamical system which depends on multiple parameters. The ROM is a projection of the dynamical system on a low dimensional space that is both problem-dependent and parameter-specific. The ROM exploits compressed tensor formats to find a low rank representation for a sample of high-fidelity snapshots of the system state. We showed that computational costs of the online phase then depend only on tensor compression ranks, but not on space or time resolution of high-fidelity computations. Moreover, certain compressed tensor formats enable to avoid the adverse effect of parameter space dimension on the online costs. The analysis of the approach includes an estimate for the representation power of the acquired ROM basis. The work was reported in a paper appeared in Computer Methods in Applied Mechanics and Engineering.

Research work during the Radcliffe fellowship year

As mentioned above, Quaini has been the 2021-22 William and Flora Hewlett Foundation Fellow at the Harvard Radcliffe Institute during Year 2 of this project. The overall goal of her Radcliffe project is to reduce the computational time of weather (and eventually climate) predictions and ocean modeling. So far, this resulted in the following publications that acknowledge this NSF grant as well:

- A paper appeared in the Journal of Advances in Modeling Earth Systems on the use of fully nonstructured grids for Kessler's microphysics with warm rain. On the left, a snapshot of a supercell thunderstorm simulation with a grid of unstructured hexahedra.

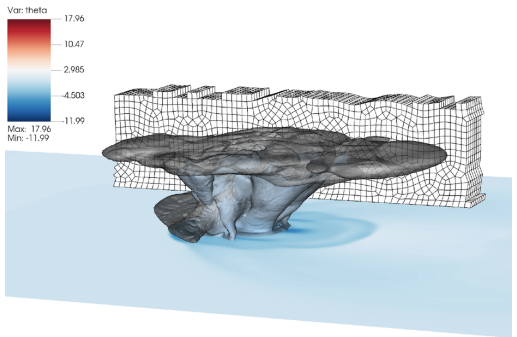

Mesh resolution	#CPUs	Wall clock	CPU hrs	Physical time
250 m	40	168 hrs	6720	2 hrs

- A paper appeared in AIP Advances on the validation of an OpenFOAM-based solver for the Euler equations with benchmarks for mesoscale atmospheric modeling.
- A paper about to be submitted on filter stabilization for the mildly compressible Euler equations with application to atmosphere dynamics simulations.

Research work during the Radcliffe fellowship year

- A paper appeared in Computers & Fluids on a POD-Galerkin reduced order model for the Navier-Stokes equations in stream function-vorticity formulation. Below figures from a vortex merger test in the North Atlantic Ocean: initial vorticity (left), vorticity after 100 time units (center), and computational mesh (right).

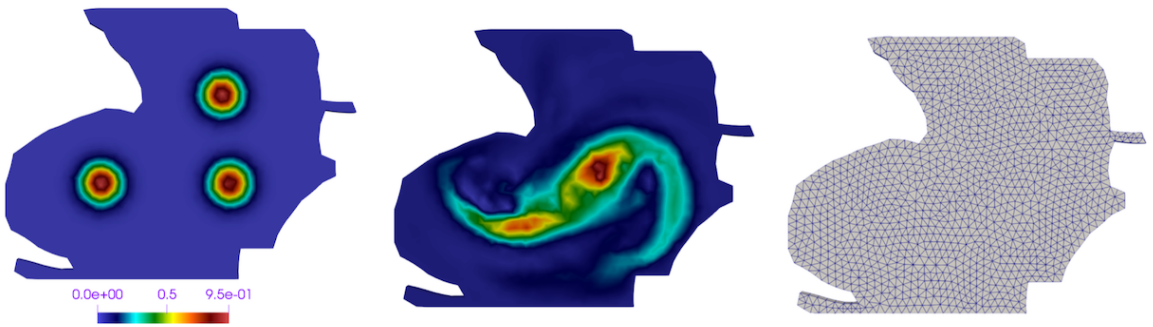

- A paper appeared in the Journal of Computational and Applied Mathematics on a LES model for the quasi-geostrophic equations in a finite volume setting. PhD student Lander Besabe is working on an extension of the LES model to the two-layer quasi-geostrophic equations.
- A paper appeared in Comptes-Rendus Mécaniques on a linear filter regularization for POD-based reduced order models of the quasi-geostrophic equations.

Open-source library

All the software created for the papers mentioned in the previous two slides is released through a new open source package called GEA (Geophysical and Environmental Applications) available to the scientific community through github:

`https://github.com/GEA-Geophysical-and-Environmental-Apps/GEA`

We chose to base GEA on finite volume C++ library OpenFOAM®, which is widely used in CFD. Thanks to parallel computing support, multiphase modeling capabilities, a wide range of existing turbulence models and ease of implementation for new ones, OpenFOAM represents a great tool for the development and assessment of computational strategies for atmospheric and ocean modeling.

Plans for the Next Reporting Period

- Deployment of the solver created for the previous point to quantify the uncertainty in the simulations and estimate the likelihood of a liposome with a given composition to fuse with a cell membrane.